Analysis of solution structure of isolated lignins and their related compound with size-exclusion chromatography equipped with multi-angle light scattering detector

(光散乱検出器を備えたサイズ排除クロマトグラフィーを用いた単離リグニン及び関連化合物の溶液構造の解析)

Linping Wang

Doctoral thesis

Supervisor: Professor Yasumitsu Uraki

Laboratory of Wood Chemistry
Division of Environmental Resources
Graduate School of Agriculture
Hokkaido University

Sapporo 2020

Contents

Chapter 1. Introduction 1

1.1. What is lignin? 1

1.1.1. Lignin biosynthesis and its chemical structure 1

1.1.2. Native lignin and technical lignin 5

1.1.3. Utilization of lignin 8

1.2. Molar mass determination of lignin 9

1.2.1. SEC equipped with ultraviolet (UV) and reflective index (RI) detectors 10

1.2.2. Mass spectroscopy 12

1.2.3. NMR end group titration 13

1.3. SEC equipped with multi-angle laser-light scattering detector (SEC-MALS) 14

1.3.1. SEC-MALS for lignin MM determination 17

1.3.2. Light absorption and fluorescence 18

1.4. Research objectives 20

1.4.1. Summary of Chapter 2. -Effect of MALS laser wavelength on lignin MM determination- 21

1.4.2. Chapter 3. -Relationship between branched structure and MM- 21

Chapter 2. Determination of acetylated hardwood kraft lignin via SEC-MALS using different wavelength laser light 23

2.1. Introduction 23

2.2. Experimental 24

2.2.1. Preparation and fractionation of HKL 24

2.2.2. *dn*/*dc* measurements 25

2.2.3. Determination of molar mass (MM) and molar mass dispersity ($Đ_M$) by SEC-MALS 26

2.2.4. Establishment of Mark-Howink-Sakurada equation 27
2.3. Results and discussion 28
2.3.1. Solvent fractionation of HKL 28
2.3.2. Determination of *dn*/*dc* 29
2.3.3. Validity of SEC-MALS analysis using two MALS lasers at different wavelengths 30
2.3.4. MM and $Đ_M$ of HKL and its fractions 32
2.3.5. Establishment of the parameters, k and a, in Mark-Houwink-Sakurada equation for HKL 37
2.4. Conclusion 40

Chapter 3. Relationships between MM of lignin and its branched structure 41

3.1. Introduction 41
3.2. Experimental 42
3.2.1. Sample preparation for the SEC-MALS analysis 42
3.2.2. MALDI-TOF MS measurement 43
3.2.3. Determination of MM by SEC-MALS 44
3.2.4. Calculation of hydrodynamic radius for Ac-HKL, Ac-SKL and Ac-M-8O4’ 44
3.2.5. Quantification of the 5-5’ interunit linkage of lignins and their fractions .. 46
3.3. Results and discussion 48
3.3.1. SEC-MALS measurement of three acetylated lignin samples 48
3.3.2. Determination of the frequency of 5-5’ linkage in lignins and their fractions 52
3.3.3. Relationship between lignin MM and 5-5’ abundance 57
3.4. Conclusion 58

Chapter 4 Conclusions 60

4.1. Summary of this study 60
4.2 General discussion and outlook 62

References.....64

Acknowledgement 76

Chapter 1. Introduction

1.1. What is lignin?

Lignin, an aromatic polymer composed of phenylpropane units, is the second most abundant biomass component after cellulose in terrestrial plants. Its content depends on the wood types and accounts for ~30% and ~20% of the dry matter in softwood and hardwood, respectively (Diamel 2010). The main biological function of lignin in the plants is considered to enhance the mechanical strength of plant cell wall, to provide waterproof for cellulose in order to assist water transportation in conducting tissue and to protect the cell wall from the microbial and fungal infection (Bellaloui et al. 2012; Campbell and Sederoff 1996).

1.1.1. Lignin biosynthesis and its chemical structure

Lignin consists of three basic phenylpropane monomers, *p*-coumaryl alcohol (p-hydroxyphenyl unit, H-type), coniferyl alcohol (guaiacyl unit, G-type) and sinapyl alcohol (syringyl unit, S-type), as shown in Figure 1-1. They are termed as monolignols. In lignin nomenclature, the aromatic carbon attached to the aliphatic chain is numbered as C-1, while the phenol carbon is numbered as C-4. The three carbons in aliphatic chain are numbered as C-7, C-8 and C-9 from the aromatic ring, which correspond to α, β and γ carbons, respectively, in classic nomenclature of lignin chemistry. In general, softwood (gymnosperm) lignins consist mainly of G-units with a low content of H-units (< 10%), whereas hardwood (angiosperm) lignins are composed principally of G- and S-units and traces of H-units. Lignins from grasses (monocots) contain G- and S-units at comparable levels, and more H-units (1-15 %) than

hardwood lignin (Baucher et al. 1998; Boerjan et al. 2003). By free-radical oxidative coupling, these free monolignols are polymerized into lignins.

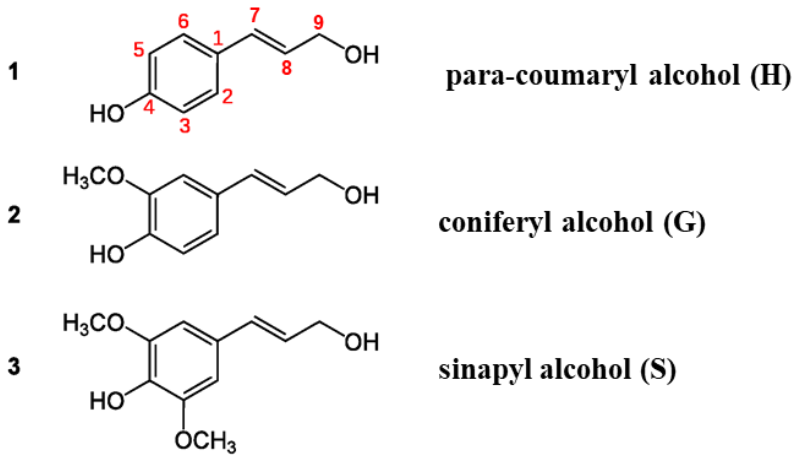

Figure 1-1. Structure of monolignols.

Herein, a radical coupling as a final process of lignin formation is elucidated by using coniferyl alcohol as an example of monolignols. Figure 1-2 shows a radical resonance consisting of the 5 types of mono-radical generated by the enzymatic hydrogen abstraction at the initiation step of lignin biosynthesis. First, coniferyl alcohol is oxidized by peroxidases/H_2O_2 or oxidases/O_2, and forms a phenolic radical (O4-radical) (Baucher et al. 1998; Higuchi and Ito 1958). Then, the unpaired electron (radical) at O-4 position resonates and localize at C-1, C-3, C-5 and C-8 positions. These radicals can form at least 9 types of interunitary linkage, as shown in Figure 1-3. The proportions of these interunitary linkages were listed in Table 1-1. Among these interunitary linkages, *8-O-4'* bonding is the most abundant, around 50% for softwood and 60% for hardwood. The next abundant linkages are *8-5'* and *5-5'*. The linkages of *4-O-5'* and *5-5'* can be branching points of lignin chain. Therefore,

unlike cellulose, which is linear and consists of only one type of monomer (glucose) and one type of interunit linkage (*β→1,4*), lignin has a quite complicated structure.

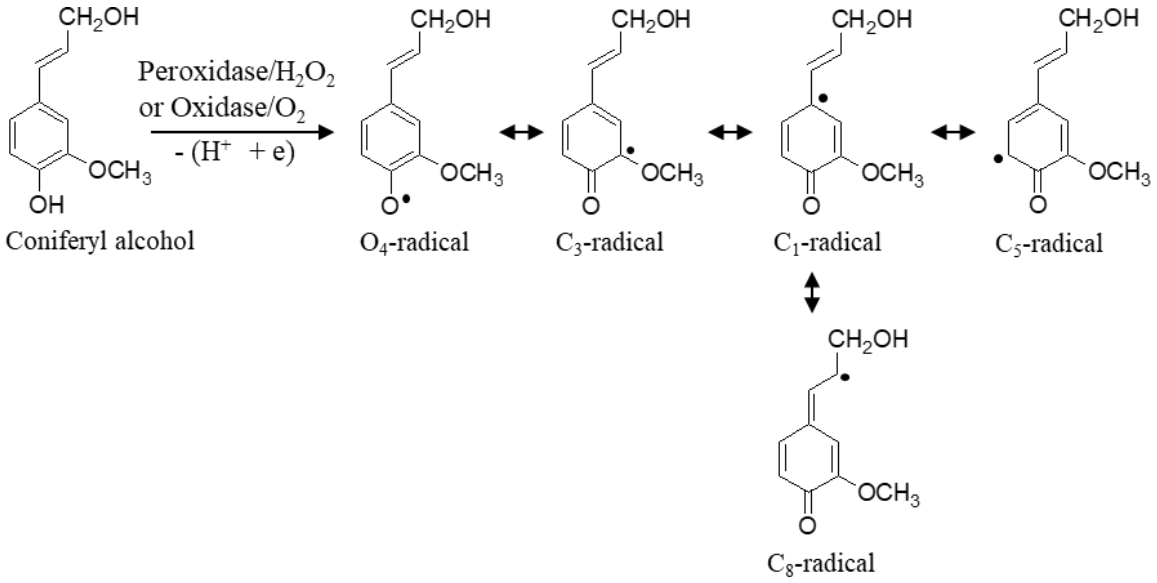

Figure 1-2. Hydrogen abstraction and radical resonance of resultant monoradical from coniferyl alcohol at the initial step of lignin biosynthesis in softwood.

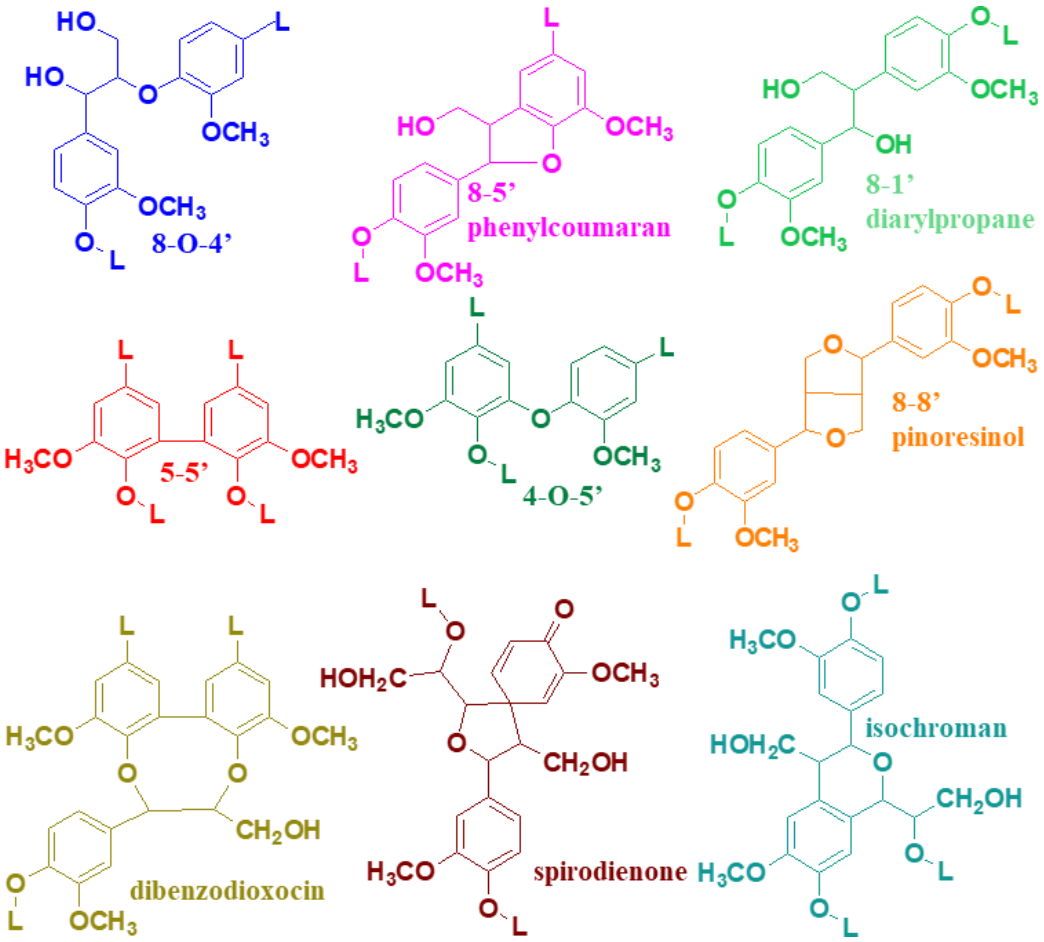

Figure 1-3. Interunitary linkages of lignin.

Table 1-1. Proportions of different types of lignin interuniatry linkages (Sjostrom 1993).

Linkage type	Dimer structure	Percent of the total linkages	
		Softwood	Hardwood
8-*O*-4'	Arylglycerol-8-aryl ether	50	60
7-*O*-4'	Noncyclic benzyl aryl ether	2-8	7
8-5'	Phenylcoumaran	9-12	6
5-5'	Biphenyl	10-11	5
4-*O*-5'	Diaryl ether	4	7
8-1'	Diaryl propane	7	7
8-8'	Linked through side chains	2	3

1.1.2. Native lignin and technical lignin

To study the structure of lignin, the lignin types should be clarified first. The lignin in its original form present in the cell walls of plant or lignocellulose is named as “native lignin” (Shrotri et al. 2017). As there are many covalent bonds between carbohydrate and lignin, isolation of the native lignin from biomass without any structural damage is still a big challenge. Therefore, among lignins isolated from lignocellulose, “milled wood lignin (MWL)”, which is separated by the means of ball milling followed by solvent extraction (Björkman 1954), are used as a near-native lignin as well as cellulolytic enzyme lignin (CEL) (Chang et al. 1975) and enzymatic mild acidolysis lignin (EMAL) (Wu and Argyropoulos 2003). Table 1-2 shows the similarities and differences in the key procedures to prepare these three isolated lignins. The step of ball milling is needed for preparation of all near-native lignins. Although this step decreases the molar mass, increases the α-carbonyl and phenolic hydroxy content, and changes the syringyl/guaiacyl (S/G) ratio of lignin (Capanema et al. 2015; Chang et al. 1975), the structure of the obtained lignin is considered to be not severely changed. Thereby, MWL, CEL and EMAL are often used as representative isolated lignins instead of native lignin. As the preparation processes of these near-native lignins are time-consuming, the obtained lignins are only used for academic research.

Table 1-2. Similarities and differences of the key procedures to prepare MWL, CEL and EMAL.

Key procedure	MWL	CEL	EMAL
Ball Milling	○	○	○
Enzymatic hydrolysis		○	○
Extraction with 96% (v/v) dioxane	○	○	
Extraction with 50% (v/v) dioxane		○	
Reflux with acidic 85% (v/v) dioxane at 86 °C			○

Another type of isolated lignins is degraded lignins produced from the pulping process, which is called "technical lignins" to differentiate them from the native and near-native lignins. Currently approximately 50-100 million tons of technical lignins are annually produced as a major component of black liquor from the pulping industry (Bajwa et al. 2019). Based on the pulping method, there are four major types of technical lignin: kraft lignin, soda lignin, lignosulfonate and organosolv lignin.

Kraft pulping is now the most popular pulping process in the world. The key chemicals used are sodium hydroxide and sodium sulfide. The native lignin within the cell wall is degraded by the reagents to dissolve in the alkaline pulping liquors. Phenylcoumaran (*8-5'*) and *8-1'* interunitary linkage in lignin are easily attacked by HO^- or HS^-, and transformed into a conjugated structure like stilbene. Repolymerization of phenolic radicals occurs during this process. There are several commercialized kraft lignins like Indulin AT (pine kraft lignin, produced by Mead Westvaco Corp., USA) and BioChoice™ lignin (pine kraft lignin, produced from LignoBoost process by Domtar Corp., USA).

Soda lignin is produced from the soda pulping process with the sodium hydroxide used

as the cooking chemical. In general, anthraquinone (AQ) is added as a pulping catalyst to decrease the carbohydrate degradation and to accelerate the cleavage of *8-O-4'* linkage. The redox cycle between AQ and the reduced form anthrahydroquinone (AHQ) can effectively cleavage the *8-O-4'* ether linkages in lignin. Compared to kraft lignin, soda lignin is more condensed as it is sulfur-free and there is no thiol groups blocking the reactive benzylic centers (Macfarlane et al. 2014). Protobind™ 1000 (grass soda lignin from a mixture of wheat/Sakanda) is one commercialized soda lignin produced by GreenValue S.A. (Switzerland).

Lignosulfonate is produced from sulfite pulping. The pulping was the most popular pulping method until 1970s. The key pulping chemical is sulfite or bisulfite salts. During the delignification process, lignin is modified to introduce sulfate esters as an anionic moiety. Thus, the resultant lignosulfonate is water-soluble, and acts as an anionic polyelectrolyte. SAN X®, VANILLE X® and PEARLLE X® are commercialized lignosulfonate products supplied from Nippon paper Industry (Japan).

Organosolv lignins are produced by the solvolysis of lignocellulose with several organic solvents and/or mixtures of organic solvents and inorganic chemicals at evaluated temperature in the typical range of 170-220 ^{o}C. There are reported many solvents for the pulping, such as methanol, ethanol, butanol, glycol, acetic acid and so on. As the inorganic chemicals, alkali hydroxides (KOH and NaOH) and mineral acids (HCl and H_2SO_4) are widely used as a catalyst to accelerate delignification. An example of the mixture is MeOH-NaOH system (Johansson et al. 1987). A well-known organosolv lignin is “Alcell lignin” preparedredred from ethanol–water pulping process.

1.1.3. Utilization of lignin

Although large amounts of technical lignins are produced as by-products every year, their industrial applications are very limited. Around 98% of the technical lignins are just burned to utilize them as fuel in the pulping mill, and only less than 2% of the technical lignins is sold and used for producing chemicals like dispersants, adhesives and surfactants. Around 88% of the sold technical lignin is lignosulfonates, which were widely used as a water reducer in making concrete last century (Bajwa et al. 2019). So far, no high value-added industrial application of technical lignins except for lignosulfonate is achieved.

On the other hand, high value-added utilizations of technical lignins have been intensively studied at lab scale. As the technical lignins have larger carbon content than cellulose, they are widely studied as the carbon fiber precursor (Kadla et al. 2002; Norberg et al. 2013; Sudo and Shimizu 1992; Uraki et al. 1995; Wang et al. 2017; You et al. 2015). As technical lignins also have lots of aliphatic and phenolic hydroxy groups, they are also widely studied as polyol for synthesis of polyurethane (Culebras et al. 2018; Hatakeyama et al. 2003; Liu et al. 2019), phenolic resin (Muller et al. 1984; Pang et al. 2017; Sarkar and Adhikari 2000), epoxy resin (Hofmann and Glasser 1993; Nagatani et al. 2019; Sasaki et al. 2013) and polyester (Kaneko et al. 2010; Taira et al. 2019). In addition, from the viewpoint of an aromatic polymer, the lignins are feed-stocks of some aromatic compounds, like vanillin, benzene, toluene and xylene (Araújo et al. 2010; Ragauskas et al. 2014). In fact, vanillin was produced from the black liquor of sulfite pulping via alkaline oxidation until 1980's. However, except for vanillin production, other high value-added utilizations of technical lignins have not been achieved at industrial scale. The main reason is the chemical structural inhomogeneity of technical lignins.

Their structures vary with their wood species, geographic environment, pulping method and pulping conditions. Nowadays, with the development of NMR techniques, the hydroxy content, types and frequencies of interunitary linkages can be determined by ^{31}P NMR and 2D NMR (Capanema et al. 2001; Crestini et al. 2017). However, measurement of accurate molar mass (MM), which is a very important chemical parameter for lignin characterization, has not been established.

1.2. Molar mass determination of lignin

A recognition to isolated lignins and their MM has changed over the last few decades. Some studies show that lignin is oligomer, which contains only 8 to 10 repeat units (Crestini et al. 2011), while other studies show that lignin is macromolecule (Chang et al. 1975; Gidh et al. 2006). Such discrepancy is assumed to be attributed to the different lignin MM determination method.

There are many methods have been applied to determine the MM of lignin. Before the 1980s, the weight-average MM (Mw) of isolated lignin was determined by light scattering (Moacanin et al. 1955; Woerner and Mccarthy 1988) and sedimentation equilibrium under analytical ultracentrifugation (Chang et al. 1975; Rezanowich et al. 1964); The number-average MM (Mn) was determined by vapor pressure osmometry (VPO) (Brown 1967; Dolk et al. 1986; Siochi et al. 1990) and cryoscopy (Chuksanova et al. 1961; Gross et al. 1958; Powell and Whittaker 1924). In the last three decades, size-exclusion chromatography (SEC), mass spectroscopy and NMR end-group titration were used to determine the lignin MM. The information of each method is shown in Table 1-3.

Table 1-3. Typical MM determination method (Umoren and Solomon 2016).

Technique	Type of MM	MM range / g mol^{-1}
Light scattering	Mw	10^2-10^8
Sedimentation equilibrium	Mw	$<10^6$
Vapor pressure osmometry	Mn	$<10^4$
Cryoscopy	Mn	$<10^4$
SEC	Mw, Mn, Mz	10^2-10^7
SEC-MALS	Mw, Mn, Mz	10^2-10^8
MS	Mn	$<10^5$
End group analysis	Mn	$<10^5$

1.2.1. SEC equipped with ultraviolet (UV) and reflective index (RI) detectors

Among all the MM determination methods, SEC connected with ultraviolet (UV) detector or reflective index (RI) detector is most widely used. SEC separates the molecules based on their size, i.e. hydrodynamic volume, by filtration through the columns, which are filled with beads containing many pores with a specific diamter distribution. When small molecules diffuse into these pores of column, their flow through the column is retarded. By contrast, large molecules, which do not enter the pores, are eluted at the void volume of the column. Consequently, by SEC separation, larger molecules are eluted earlier than smaller molecules. The elution of molecules from the column is generally detected by using a RI detector, but an UV detector is wider used for lignin because it is more sensitive for lignin than RI detector. Afterwards, Mn, Mw and peak MM (Mp) of the specimen are calculated by using calibration curves. There are two types of calibration curve. One is a conventional calibration

curve, which plots log M against elution volume (Mourey et al. 1990), where M is the MM of the standard molar mass maker. In this measurement, only the relative MM of specimen is obtained instead of the absolute MM, because this calibration curve does not involve in the information of hydrodynamic volume. Therefore, only when the hydrodynamic volume of specimen is identical to the standards at the same retention time, the obtained relative MM is near to the absolute MM. The other calibration curve is "universal calibration curve", which plots the log [η]M against the elution volume (Grubisic et al. 1967; Guo et al. 2003; Weiss and Cohn‐ginsberg 1969), where [η] is the intrinsic viscosity of specimen, and a measure of the hydrodynamic radius. This measurement is appliable to obtain the absolute Mn and Mw for any unknown polymers. However, the [η] determination is a tedious process. Currently SEC combined with the conventional calibration curve is, therefore, widely used to determine MM.

When using the SEC method combined the conventional calibration curve for lignin preparations, authentic polystyrene is used as a marker material of MM for making conventional calibration curve, and tetrahydrofuran (THF) is widely used as an eluent for acetylated lignins (Baumberger et al. 2007; Glasser et al. 1993; Siochi et al. 1990).

1.2.1.1. Invalidity of polystyrene for the molecular maker for lignin

[η] of kraft lignin in dioxane was 0.06 dl g^{-1} (Lindberg et al. 1964), and that of polystyrene in dioxane was 1.13 dl g^{-1}(Chee 1987), suggesting that hydrodynamic volume of kraft lignin in dioxane was much smaller than that of polystyrene. The low [η] value of kraft lignin was attributed to low value of exponent "a" in Mark-Houwink-Sakurada equation ([η]=KM^a). When $a \leq 0.5$, it means the polymer has dense solution structure; when $0.5 \leq a \leq 0.8$, the polymer has

flexible solution structure. According to the reported studies, [η] and exponent "a" (0.12-0.32) of several isolated lignins in alkaline aqueous solution and organic solvents were much lower than those of synthetic polymers (Goring 1971). These results suggest that the conformation of isolated lignins in any solvent is very compact like Einstein's sphere. Although there was no report on [η] and exponent "a" of any isolated lignins in THF, they are expected to be much lower than those ([η], 0.102-2.29 dl g^{-1}; a, 0.725) of polystyrene in THF (Alliet and Pacco 1968; Spatorico and Coulter 1973). Therefore, polystyrene is not suitable as a marker for MM determination of lignin, and the obtained MM of lignin calculated from the conventional SEC method must be much smaller than the absolute MM.

1.2.2. Mass spectroscopy

For MM determination of macromolecule, matrix-assisted laser desorption ionization time-of-flight mass spectroscopy (MALDI-TOF MS) is frequently used, especially for biomacromolecules like DNA and protein. In this measurement, a specimen is mixed and co-crystalized with a matrix material, and then a laser flash ionizes the matrix material. Finally, a mass-to-charge ratio of specimen ion is determined via the time-of-flight measurement. Several studies of lignin MM determination with MALDI-TOF MS are reported to use 2,5-dihydroxybenzoic acid (DHB) as a matrix material. (Jacobs and Dahlman 2000; Metzger et al. 1992; Rönnols et al. 2017). One problem is that the matrix, structurally similar o lignin, increased the background and complexity of the MS spectrum. Hence, laser desorption ionization time-of-flight mass spectroscopy (LDI-TOF-MS) without using matrix materials is

used for lignin MM determination (Andrianova et al. 2018). However, both MALDI-TOF MS and LDI-TOF MS have an obvious problem that the ionization of high MM lignin molecules is suppressed compared to that of the low MM fractions. Therefore, this application is only limited to lignin fractions as a oligomer size with a narrow molar mass dispersity ($Đ_M$) (Jacobs and Dahlman 2000).

1.2.3. NMR end group titration

NMR is a powerful technique to analyze the bonding mode and function group of lignin. It can be used for MM determination method when the content of the polymer end group and the repeat unit structure are obtained. According to Crestini et al.'s work (Crestini et al. 2011), the end group of MWL is identified as the phenolic hydroxy. When a lignin chain contains only *8-O-4'* and *8-5'* interunitary linkage, this chain has only one phenolic hydroxy group. In addition, when a lignin chain contain one *8-8'*, *8-1'* or *5-5'* interunitary linkage, the phenolic hydroxy number of this chain is increased by one. Therefore, the number of lignin chains is equal to the total phenolic group abundance subtracting the *8-8'*, *8-1'* and *5-5'* abundance, which were estimated by ^{31}P NMR and 2D NMR analysis. Then, the degree of polymerization (DP) is calculated according to the number of lignin chains, and the final Mn is calculated by multiplying DP and the average MM of the repeating unit. However, as technical lignins undergo severe degradation and repolymerization reactions, their interunitary bonds are more complicated than MWL, and it is difficult to find the relationship between the abundance of phenolic hydroxy and the chain number. Furthermore, it is considered that there are no clear

repeating units of technical lignins. Therefore, NMR end group titration cannot be used for MM determination of technical lignins.

1.3. SEC equipped with multi-angle laser-light scattering detector (SEC-MALS)

Currently, SEC combined with multi-angle laser-light scattering detector (SEC-MALS) is widely used for the MM determination of some polysaccharides, such as cellulose (Dupont and Harrison 2004; Ono et al. 2015), hemicellulose (Chemin et al. 2015; Kleen et al. 2016), starches (Han and Lim 2004) and hyaluronic acid (Hokputsa et al. 2003). This combined analyzing method enables to obtain the absolute Mn, Mw and molar mass dispersity ($Đ_M$) without a calibration curve created from MM makers. To better understand the mechanism of SEC-MALS, firstly, the theory of Mw determination by MALS is explained. In a MALS detector, the intensity of the incident laser (I_0) light is detected by a laser monitor, and the transmitted light (I_t) is detected by a forward monitor as shown in Figure 1-4-A. When the incident light meets specimen in a measurement cell, Rayleigh scattering occurs, and the scattered intensity is detected by the photodiodes at different angles. Figure 1-4-B and C show the specific position of each photodiode in two different MALS detectors which are used in this study. One is with 8 photodiodes, the other is with 18 photodiodes. These photodiodes can detect the light at any wavelength. According to the intensity of the Rayleigh light scattering, Mw is calculated based on Eq 1-1, 2 and 3.

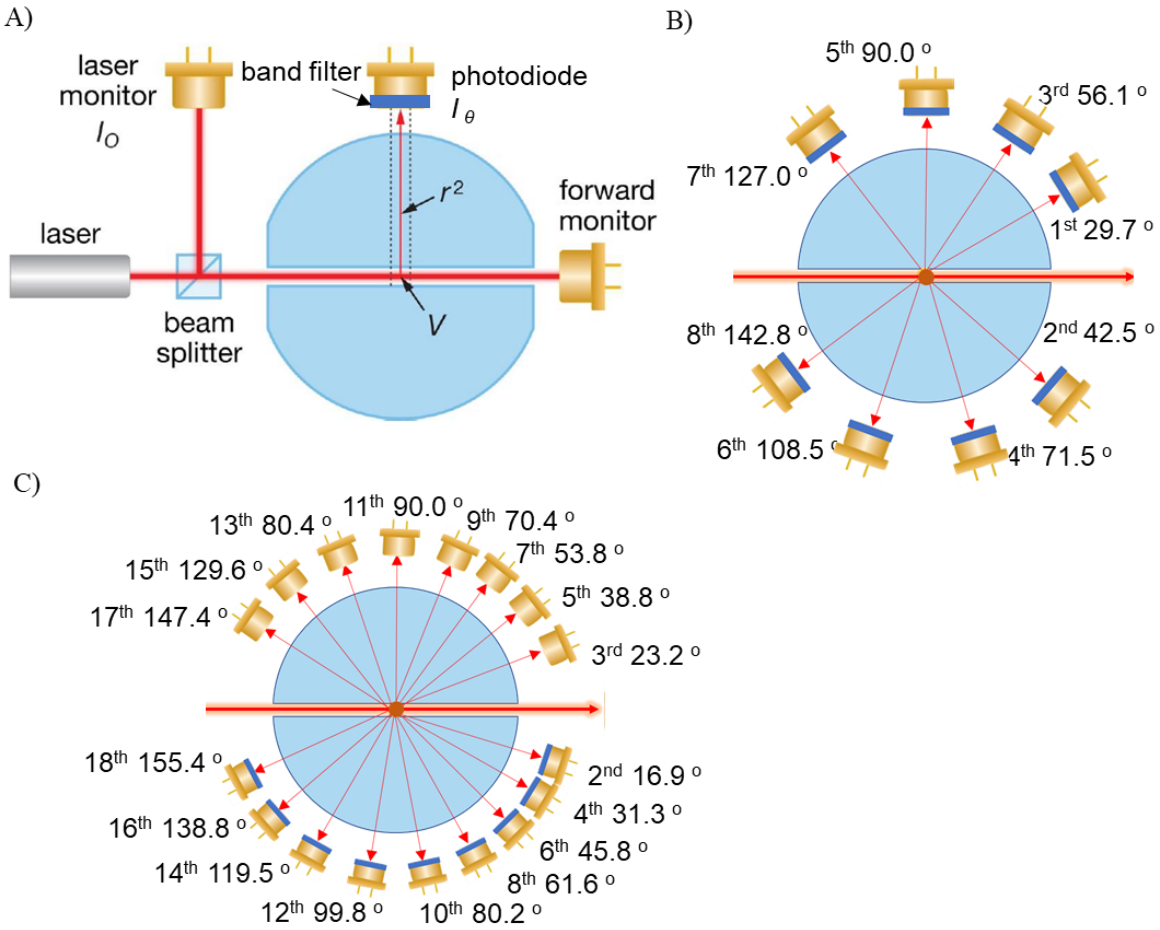

Figure 1-4. Illustration of A) multi-angle light scattering detector and photodiodes positions in B) 8-angle MALS and C) 18-angle MALS.

$$R(\theta) = \frac{I_\theta r^2}{I_0 V} \tag{1-1}$$

$$\frac{K^* c}{R(\theta)} = \frac{1}{M_w P(\theta)} + 2A_2 c \tag{1-2}$$

$$K^* = 4\pi^2 n_0{}^2 (dn/dc)^2 / \left[\lambda_0{}^4 N_A\right] \tag{1-3}$$

$$\frac{K^* c}{R(\theta)} = \frac{1}{M_w P(\theta)} \tag{1-4}$$

where $R(\theta)$ is the excess Rayleigh ratio; I_θ is the scattered intensity at angle θ; I_0 is the incident intensity; r is the distance from the center of sample cell to photodiode; V is the illuminated volume of the scattering medium; c is a specimen concentration (g mL^{-1}); A_2 is the second virial coefficient (a measure of the solvent-solute interaction); K^* is an optical

parameter; n_0 is the solvent refractive index; dn/dC is the refractive index increment of specimen solution; N_A is Avogadro's number, and λ_0 is the wavelength of the incident laser light. $P(\theta)$ is a function depending on the scattered light's angular, which represents the gyration radius ($<Rg^2>$) of specimen molecule. To obtain physicochemical parameters (Mw, Rg and A_2) of a specimen according to Eq 1-2, the solutions at multiple concentrations (about 5 concentrations) should be separately set and measured by MALS detector. The parameters are obtained from Zimm plots as shown in Figure 1-5-A. The slope of $\theta = 0$ line gives A_2 value, and the slope of $c = 0$ line gives $<Rg^2>$, and their intercept gives Mw.

However, in the case of MM determination with SEC-MALS, the calculation is simpler. As SEC separates specimen molecules dependently on the size, the concentration of the separated fraction at each retention time (slice i) is considered to be very low ($c \rightarrow 0$), leading to that the second term in Eq 1-2 is ignored. Thus, Eq 1-2 can be modified to Eq 1-4, and the slice result is shown in Figure 1-5-B. Only one fitting line is obtained. The intercept and slop give Mw and $<Rg^2>$, respectively, and it is impossible to obtain A_2 value via SEC-MALS. Based on the absolute MM obtained at each retention time (M_i) and the number density at each retention time (N_i) detected by RI, Mn ($\frac{\sum_i N_i M_i}{\sum_i N_i}$) and Mw ($\frac{\sum_i N_i M_i^2}{\sum_i N_i M_i}$) of the specimen can be calculated. Therefore, SEC-MALS is a sophisticated and easy method to get the absolute MM.

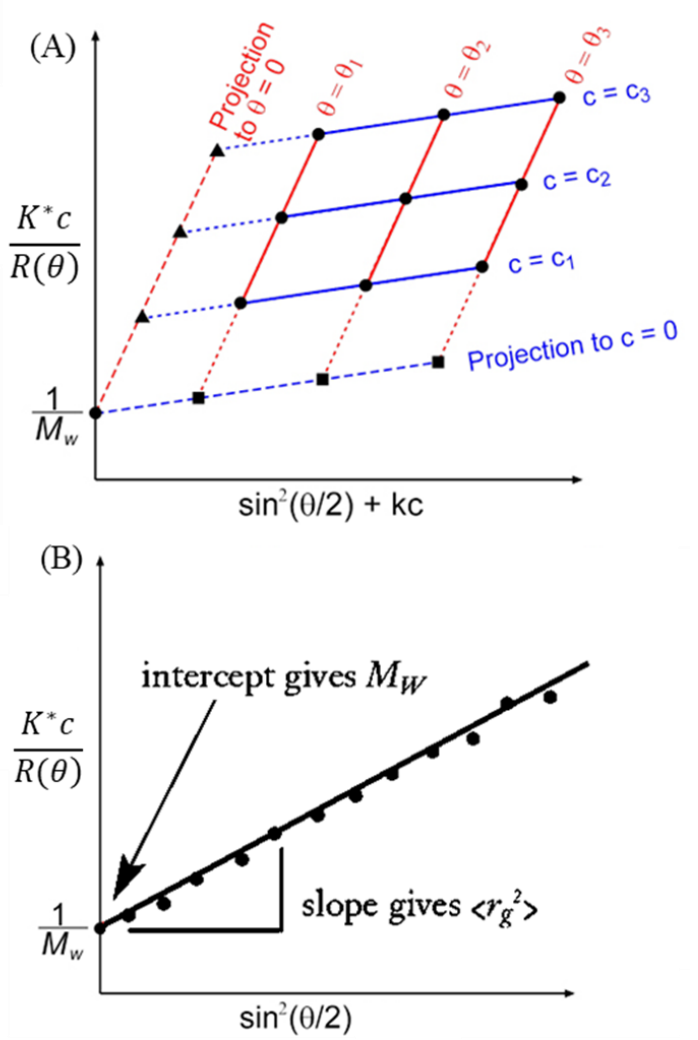

Figure 1-5. (A) Zimm plots obtained by MALS measurement; (B) Zimm plot obtained by SEC-MALS measurement.

1.3.1. SEC-MALS for lignin MM determination

Several studies of lignin MM determination with SEC-MALS have been reported in the last decade. Cathala et al. (Cathala et al. 2003) reported that the Mw of spruce milled wood lignin (MWL) was approximately 5 - 6 × 10^5 g mol^{-1} and the Mw of a dehydrogenation polymer synthesized from coniferyl alcohol was approximately 2 × 10^5 g mol^{-1}. Fredheim et al. (Fredheim 2002) reported that the Mw of Na-lignosulfonate from spruce was 6.4× 10^4 g mol^{-1}. Mikame et al. (Mikame 2006) reported that the Mw of kraft lignin and its fractions were

approximately 2.1-38.0 × 10^4 g mol^{-1} . The values were 8-28 folds lager than corresponding Mw values calculated from the conventional SEC with a conventional calibration curve. In these studies, the laser wavelengths of MALS were 633nm (Cathala et al. 2003; Fredheim 2002) and 690 nm (Mikame 2006), and the photodiode was covered with band filters, which could pass the light within a certain range of wavelength, to eliminate self-fluorescence of lignin as shown in Figure 1-4-A. However, these MALS systems involved in big suspicious: was the self-fluorescence of lignin completely removed? This self-fluorescence can cause enhancement of scattering light intensity and overestimation of MM (Contreras et al. 2008; Dong 1993; Gidh et al. 2006), which is discussed in the next section.

1.3.2. Light absorption and fluorescence

The bandwidth of the filters was 1–20 nm. Thereby, it has not been proved to completely remove self-fluorescence of lignin by the band filters. To solve the problem of lignin self-fluorescence, firstly, the relationship between light absorption and self-fluorescence of lignin is explained. Since lignin has many conjugated structures from aromatic system as mentioned above, it easily undergoes intermolecular electronic transition from ground state to excited state, which is caused by photon absorption. Then, part of this absorbed photons are emitted at longer wavelength as fluorescence radiation, when the excited electron returns to the ground state. This process is illustrated as a simplified Jablonski diagram in Figure 1-6. In this figure, S_0 is the singlet ground electronic state with a pair of electrons having opposite spins. S_1 is the 1^{st} singlet excited electronic states. S_2 is the 2^{nd} singlet excited electronic states. T_1 is the 1^{st} triplet

excited electronic states with a pair of electrons having same spin, h is Planck's constant, 6.63 x 10^{-34} J, and *v* is frequency of the light.

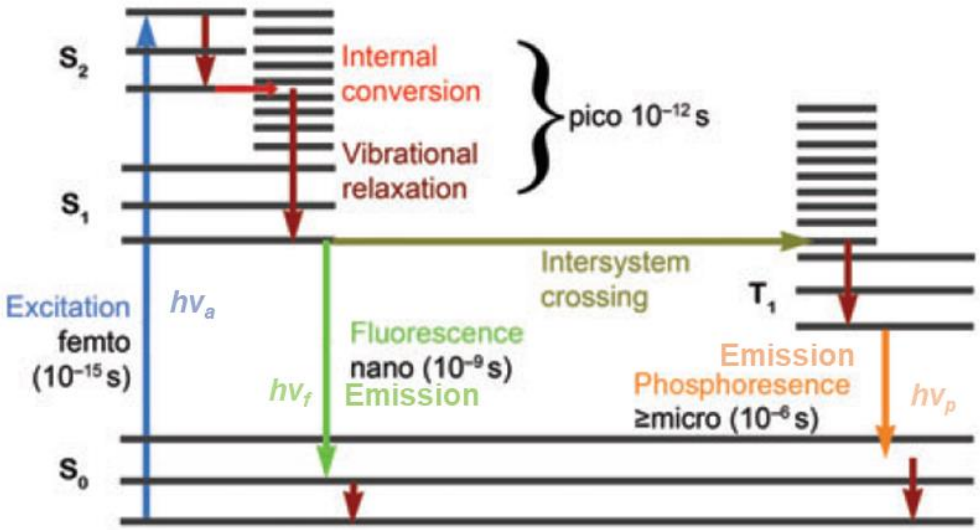

Figure 1-6. Simplified Jablonski diagram depicting the excitation of an electron by absorption of a photon (hv_a) to higher electronic states S_1, S_2 or T_1. Fluorescence is observed with the release of photon (hv_f) when the electron returns to S_0 from S_1. The electron can undergo intersystem crossing from S_1 to T_1 by changing its spin state. Phosphorescence is observed with the release of photon (hv_p) when the electron returns to S_0 from T_1. (Lichtman and Conchello 2005)

Figure 1-7 shows the typical ultraviolet (UV)-visible absorption spectra of an soda lignin solution (Singh et al. 2012) in the wavelength of 200-700 nm. High light absorbance occurs in the range of 200-250 nm, and one absorbance plateau appears near 280 nm. In the range of visible spectrum (400-700 nm), light absorbance is decreased with the increase of wavelength. Low light absorption result in low fluorescence. Therefore, a laser light at longer wavelength of more than 700 nm can minimize or eliminate the light absorption and self-fluorescence. From the background to conduct SEC-MALS for lignin, a new type of MALS system equipped

with band filters and laser light at 785 nm was recently developed and used for lignin MM determination (Yamamoto et al. 2017; Zinovyev et al. 2018).

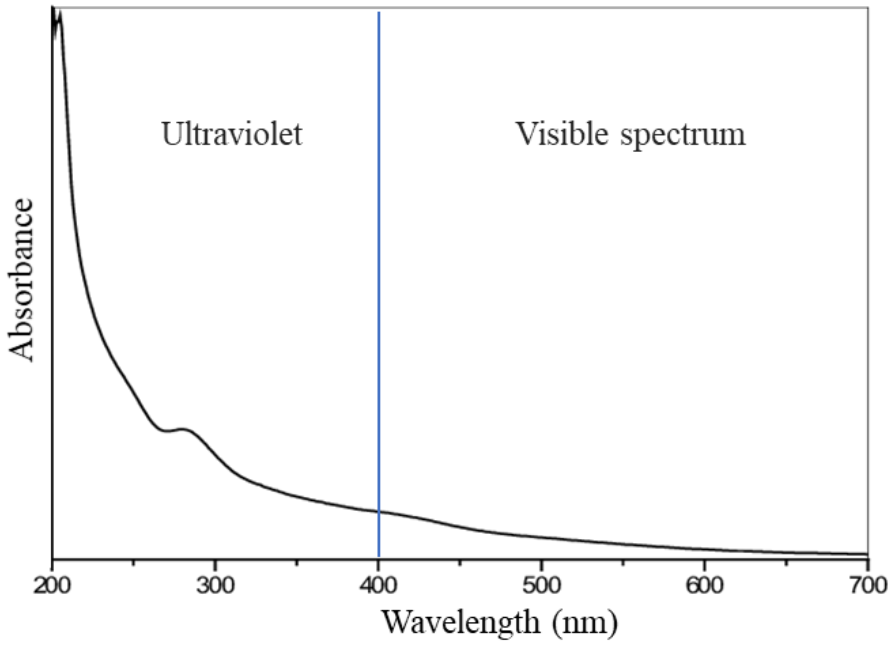

Figure 1-7. Typical UV-visible absorption spectra of lignin (Singh et al. 2012).

1.4. Research objectives

In this study, the MMs of several lignin preparations are determined via SEC-MALS method. The specimens are hardwood kraft lignin and softwood kraft lignin as technical lignins, and polymeric lignin model compound as a reference material. Firstly, the effect of laser light wavelength on lignin SEC-MALS measurement are investigated. The obtained absolute MM with SEC-MALS is compared to the relative MM calculated from the conventional SEC with a calibration curve. Secondly, the relationship between lignin MM and solution structure are investigated to further clarify the lignin property. These are described in Chapter 2 and Chapter

3. Chapter 4 is concluding remarks. A brief summary for each chapter is explained as follows.

1.4.1. Summary of Chapter 2. -Effect of MALS laser wavelength on lignin MM determination-

As mentioned in 1.3.2, the light wavelength must significantly affect the intensity of the light absorption and the self-fluorescence of lignin. In some previous studies, although the MALS equipped with laser light at the wavelength of over 600 nm and band filters, the complete elimination of lignin self-fluorescence was suspicious. In this study, the effect of laser light wavelength on MM determination of acetylated hardwood kraft lignin (Ac-HKL) was studied by using two SEC-MALS systems equipped with two different lasers at wavelength of 658 nm and 785 nm. In both two systems, THF and polystyrene-divinylbenzene resin are used as an eluent and a column-filling material, respectively.

After obtaining the absolute MM, the Mark-Houwink-Sakurada equation for Ac-HKL, exponent “a” in particular, is established from a combined result of viscosity measurement and SEC-MALS to predict the solution structure of Ac-HKL in THF. Consequently, the solution structure is compact.

1.4.2. Chapter 3. -Relationship between branched structure and MM-

To figure out why lignin molecule has a compact structure, it is proposed a hypothesis, in which the structure may come from branched chain of HKL. To confirm this hypothesis, a linear polymeric lignin model comprised of only 8-O-4’ interunitary linkage (M-8O4’) is prepared and used as non-branched lignin. Among the interunitary linkages of lignin, 5-5’ and 4-*O*-5’ are proposed to be the branching points. As 5-5’ frequency (19–27%) was much larger

than 4-*O*-5’ frequency (3.5-4%) (Chang and Jiang 2020), the abundance of 5-5’ bonding is considered as the branching frequency of these lignins. The abundance of 5-5’ biphenyl structure of KL fractions was estimated via nitrobenzene oxidation with ^{1}H-NMR spectroscopy. The relationship between branching frequencies and MMs in Ac-HKL, Ac-SKL and Ac-M-8O4’ at the same hydrodynamic radius is discussed.

Chapter 2. Determination of acetylated hardwood kraft lignin via SEC-MALS using different wavelength laser light

2.1. Introduction

Self-fluorescence of lignin causes an overestimation of lignin MM by SEC-MALS, and is significantly considered to be affected by the laser wavelength of MALS. The longer laser wavelength should cause a weaker self-fluorescence of lignin. As a result, more accurate measurement of lignin MM must be performed. So far, MALS detectors equipped with laser light at the wavelength range of 600-700 nm are widely used (Contreras et al. 2008; Gidh et al. 2006; Fredheim 2002; Mikame 2006). However, these lasers didn't completely suppress lignin self-fluorescence, particularly a band filter was not used (Contreras et al. 2008; Dong 1993; Gidh et al. 2006). In addition, the current band filter has been not clarified that it completely removes light emission due to fluorescence. Recently, a new type of MALS system with laser light at 785 nm was developed by Wyatt Corp., which is supposed to be more effective for elimination of the lignin self-fluorescence.

In this chapter, two SEC-MALS apparatuses equipped with laser lights of different wavelengths (658 nm and 785 nm) were used. Hardwood kraft lignin (HKL) was used as a measurement specimen. To further understand the solution structure or relationship between MM and hydrodynamic radius, the Mark-Houwink-Sakurada equation of Ac-HKL in THF was established based on MM of fractionated Ac-HKL.

2.2. Experimental

2.2.1. Preparation and fractionation of HKL

HKL was precipitated from a black liquor of hardwood Kraft pulping supplied by the Hainan Jinhai Pulp Paper Co., Ltd. (Danzhou, China) by acidification. The precipitate was collected by filtration and washed with distilled water until the pH of the washings reached 3. The resultant precipitate was dried in air for 48 h, and then *in vacuo* at 50 °C for 48 h to obtain the HKL powder.

HKL was fractionated according to the method reported by Cui et al. (Cui et al. 2014). The detailed procedure is shown in Scheme 2-1. Fifty grams of HKL was suspended in 500 mL of acetone with stirring for 12 h at room temperature. An acetone-insoluble fraction (AI-HKL) was separated by filtration and washed with 30 mL of acetone. The supernatant and washings were combined. Acetone was further added to the supernatant to adjust the volume to 500 mL. Hexane (125 mL) was slowly added into the acetone solution until the concentration of hexane was 20% (v/v) in the acetone solution, and the mixture was stirred for 1 h. During stirring, lignin precipitated as a gel-like material, and spontaneously adhered to the inner surface of the beaker. The precipitate was collected by decantation of the suspension and washed with a 20% (v/v) hexane in acetone to yield an acetone-soluble HKL fraction (AS-HKL 0.2). Then, hexane (209 mL) was slowly added to the supernatant of the decantation to obtain 40% (v/v) hexane in acetone, and then the mixture was stirred to generate precipitate. This precipitate was collected by the decantation followed by washing with the corresponding mixture solvent to yield the second lignin fraction (AS-HKL 0.4). All HKL fractions were dried *in vacuo* at 50 °C for 24 h.

All samples (500 mg), including unfractionated HKL, were acetylated with 10 ml acetic anhydride-pyridine (1:1, v/v) at room temperature for 48 h. The acetylated samples were precipitated by pouring the mixture into diethyl ether. The precipitates were filtered and washed with diethyl ether.

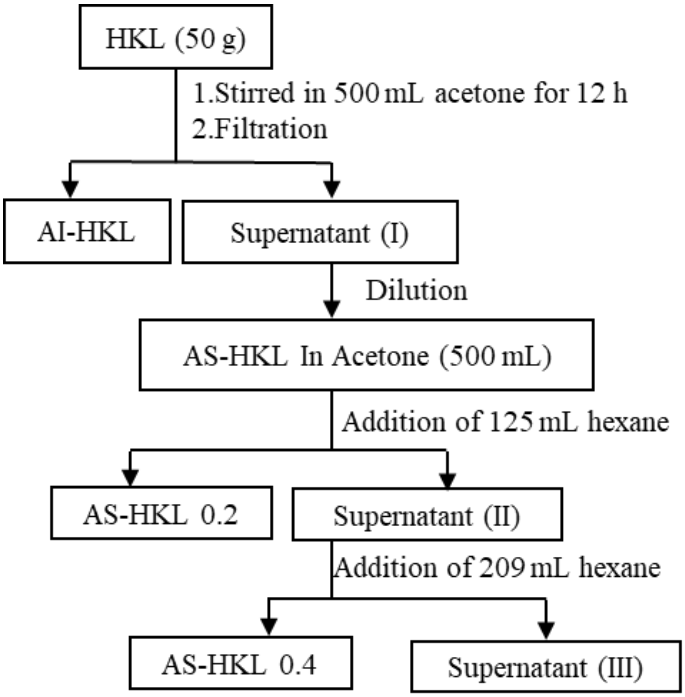

Scheme 2-1. Fractional precipitation procedure of HKL.

2.2.2. *dn*/*dc* measurements

A specific refractive index increment (*dn*/*dc*) of specimen was determined on an interferometric refractometer (Optilab T-rex, Wyatt Technology, Santa Barbara, CA, USA). The wavelength of the polarized light was 658 nm. The specimen solutions in THF at different concentrations were loaded into a flow cell of the refractometer at 25 °C at a flow rate of 0.5 mL/min. All the data were collected and processed with the ASTRA 5.3 software.

2.2.3. Determination of molar mass (MM) and molar mass dispersity ($Đ_M$) by SEC-MALS

SEC-MALS measurements were carried out with two systems. One was a high-performance liquid chromatography (HPLC) system (Agilent 1100, Palo Alto, CA, USA) equipped with a MALS detector (DAWN HELEOS- II, Wyatt Technology, Santa Barbara, CA, USA). In the detector, the wavelength of the laser light was 658 nm, and 6 of 18 photodiodes were covered with band filters to eliminate sample fluorescence. The bandwidth of the band filters was 20 nm, allowing to detect the light at wavelength of 658 ± 10 nm. This HPLC system was also equipped with a refractive index (RI) detector. In the SEC measurement, two ultra-styragel^{TM} linear columns, PL 1110-6300 (bed material: polystyrene-divinylbenzene; MM range: 0-25,000 g/mol (PS equivalent)) and PL 1110-6530 (bed material: polystyrene-divinylbenzene; MM range: 500-60,000 g/mol (PS equivalent)) from Agilent (Palo Alto, CA, USA) were connected in series. The column temperature was 25 °C, and THF was used as the eluent at a flow rate of 1.0 mL/min. The injection volume was 25 μL. A conventional calibration curve was obtained from the retention volumes of 16 authentic polystyrene standards in the MM range of 510-4,226,000 g mol^{-1}.

The other system was an HPLC system (Shimadzu LC-10, Kyoto, Japan) equipped with a MALS detector (DAWN HELEOS 8, Wyatt Technology, Santa Barbara, CA, USA). The laser light wavelength was 785 nm, and band filters with band width of 20 nm were set on all 8 detectors. An RI detector was also equipped in this HPLC system. For the SEC measurements, THF was used as an eluent at a flow rate of 0.5 mL/min. The column temperature was 35 °C, and the injection volume was 100 μL. Two identical columns (Shodex GPC KF-804 (bed material: polystyrene-divinylbenzene; MM range: 100-300,000 g/mol (PS equivalent)); Showa

Denko Co., Ltd., Tokyo, Japan) were connected in series. A conventional calibration curve was created from the retention volumes of 18 authentic polystyrene standards in the MM range of 580-4,226,000 g mol^{-1}. The Mn and Mw values from the MALS with a laser wavelength of 785 nm were calculated in the retention time range of 24-36 min by using the ASTRA 6.1 software. The relative Mn and Mw values based on the conventional calibration curve were calculated in the same retention time range.

2.2.4. Establishment of Mark-Howink-Sakurada equation

A specific viscosity (η_{sp}) and a relative viscosity (η_{rel}) of fractionated HKL at different concentrations (0.205-3.322 mg mL^{-1}) in THF and dimethyl sulfoxide (DMSO) was measured in a thermostatic water bath at 25°C by using an Ubbelohde viscometer with a viscometer factor of 0.00205 cSt/s (SU-1140, SIBATA), where η_{sp} is equal to "η_{rel}-1"; η_{rel} is equal to "t_1/t_0"; t_1 is the flow time of sample solution; t_0 is the flow time of solvent. An intrinsic viscosity ([η]) was obtained by extrapolating the linear line created by plotting η_{sp}/C against C, where C is the sample concentration. Then parameters "K" and "a" in Mark-Houwink-Sakurada (MHS) equation ($[\eta] = KM^a$, $\log [\eta] = \log K + a \cdot \log M$) were calculated from the intercept and slope of the linear fitting line of log [η] against log Mw, respectively.

2.3. Results and discussion

2.3.1. Solvent fractionation of HKL

Figure 2-1 shows the size-exclusion chromatograms of HKL and its fractions monitored by an RI detector, where the Y axis represents relative intensities to that of the highest peak, and the highest intensities of the HKL and HKL fractions were set to 2.0 and 1.0, respectively. Figure 2-1 clearly reveals that the HKL fractionated by solvent precipitation with hexane had a narrow dispersity as compared with intact HKL. AI-HKL has the largest molecular size among all fractions.

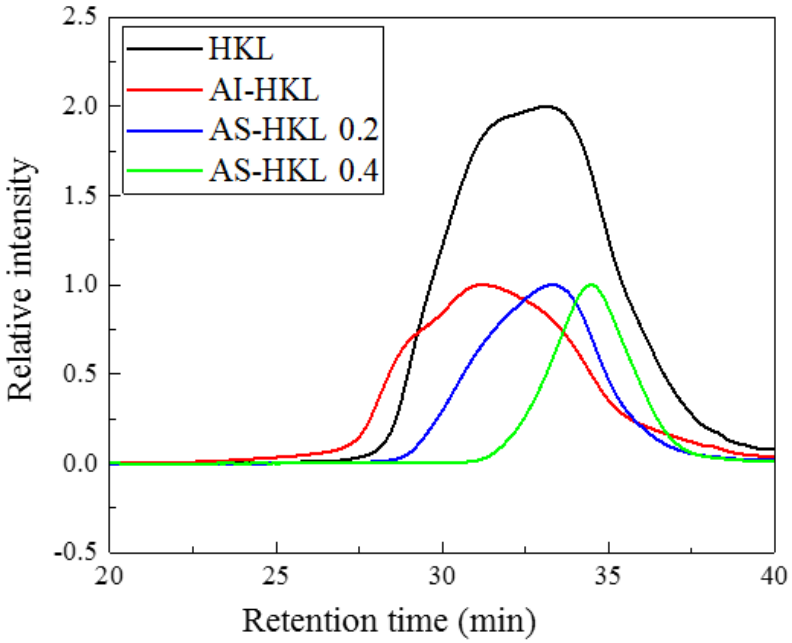

Figure 2-1. Size-exclusion chromatograms of acetylated HKL and its fractions monitored by an RI detector

2.3.2. Determination of *dn*/*dc*

Figure 2-2 shows RI values versus concentration of HKL and its fractions. Linear fitting lines with high determination coefficient values ($R^2 > 0.99$) were obtained. The *dn*/*dc* value of each sample was calculated from the slope of the fitting line and was 0.160 mL g^{-1} for HKL, 0.136 mL g^{-1} for AI-HKL, 0.165 mL g^{-1} for AS-HKL 0.2, and 0.182 mL g^{-1} for AS-HKL 0.4. This result suggests that the tendency of *dn*/*dc* increment was consistent with the increase in the MM or molecular size of HKL. In general, the *dn*/*dc* value of a homopolymer is almost identical and independent of the MM (Brandrup et al. 1999; Huglin 1965). However, the *dn*/*dc* value of a copolymer is altered depending on the MM and monomer composition (Pierre sorlier et al. 2003). Therefore, the dependence of *dn*/*dc* on the MM of HKL should be due to the copolymeric property of HKL, which is comprised of syringyl (S) and guaiacyl (G) units.

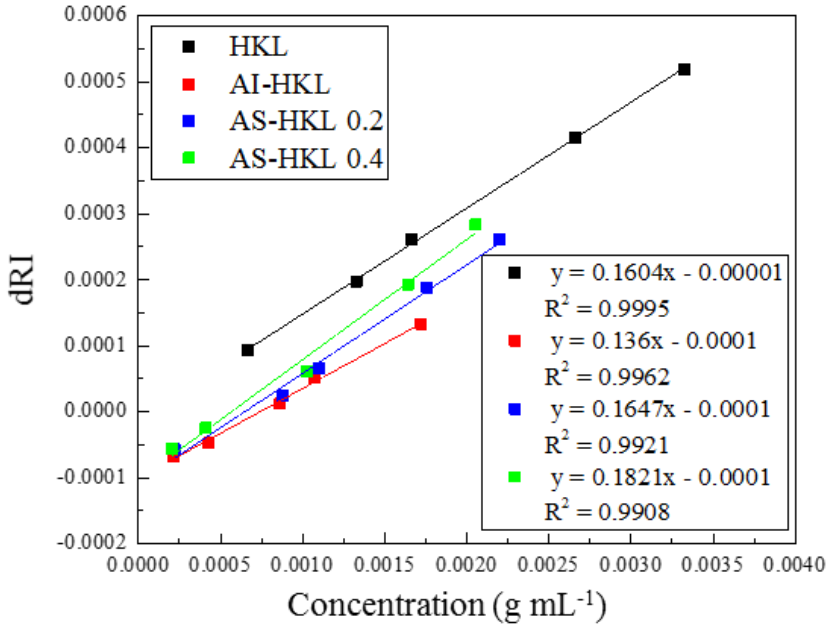

Figure 2-2. RI increments of acetylated HKL and its fractions.

2.3.3. Validity of SEC-MALS analysis using two MALS lasers at different wavelengths

Figure 2-3 shows the SE chromatograms of HKL monitored by the MALS and RI detectors, and the detector responses are represented as an output voltage. This figure contains a conventional calibration curve derived from the polystyrene standards and the absolute MM estimated by MALS with and without band filters at each retention time. Two lasers at wavelengths of 658 nm and 785 nm were used, and the corresponding chromatograms are shown in Figure 2-3-A) and B), respectively. The SEC-MALS-RI chromatograms of the HKL fractions obtained at 658 nm and 785 nm are shown in Figure 2-4.

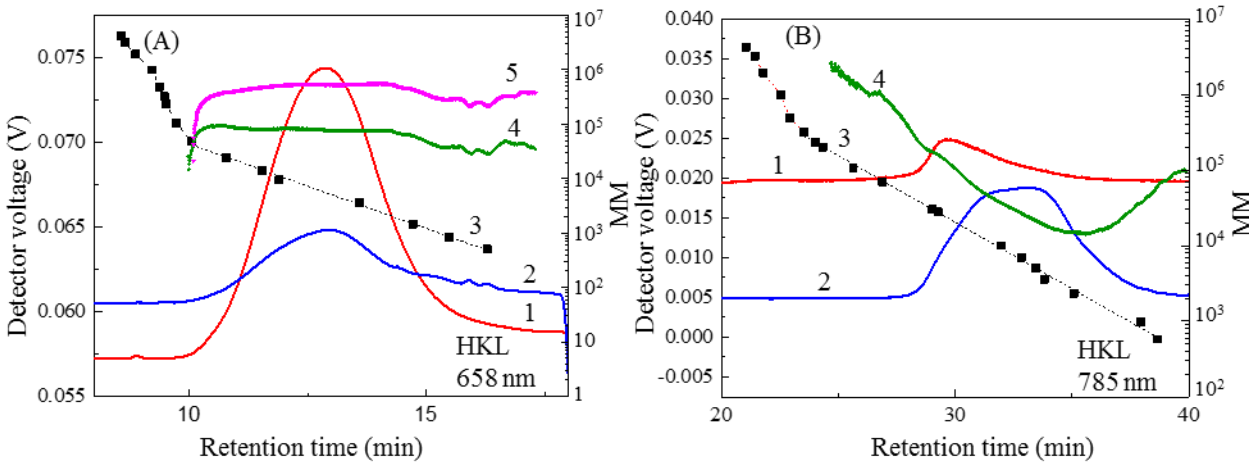

Figure 2-3. SEC-MALS-RI chromatograms of HKL obtained at 658 nm (A) and 785 nm (B). In each figure, the left Y axis represents the detector voltage for the RI and MALS responses, and the right Y axis represents the MM. Red line 1 represents the chromatograms monitored by MALS, and the detector was located at an angle of 90° from the laser light. Blue line 2 shows the chromatograms monitored by RI. Black dashed lines 3 show conventional calibration curves of polystyrene. Green lines 4 show absolute MM obtained by MALS with band filters. Pink line 5 shows absolute MM obtained by MALS without band filter.

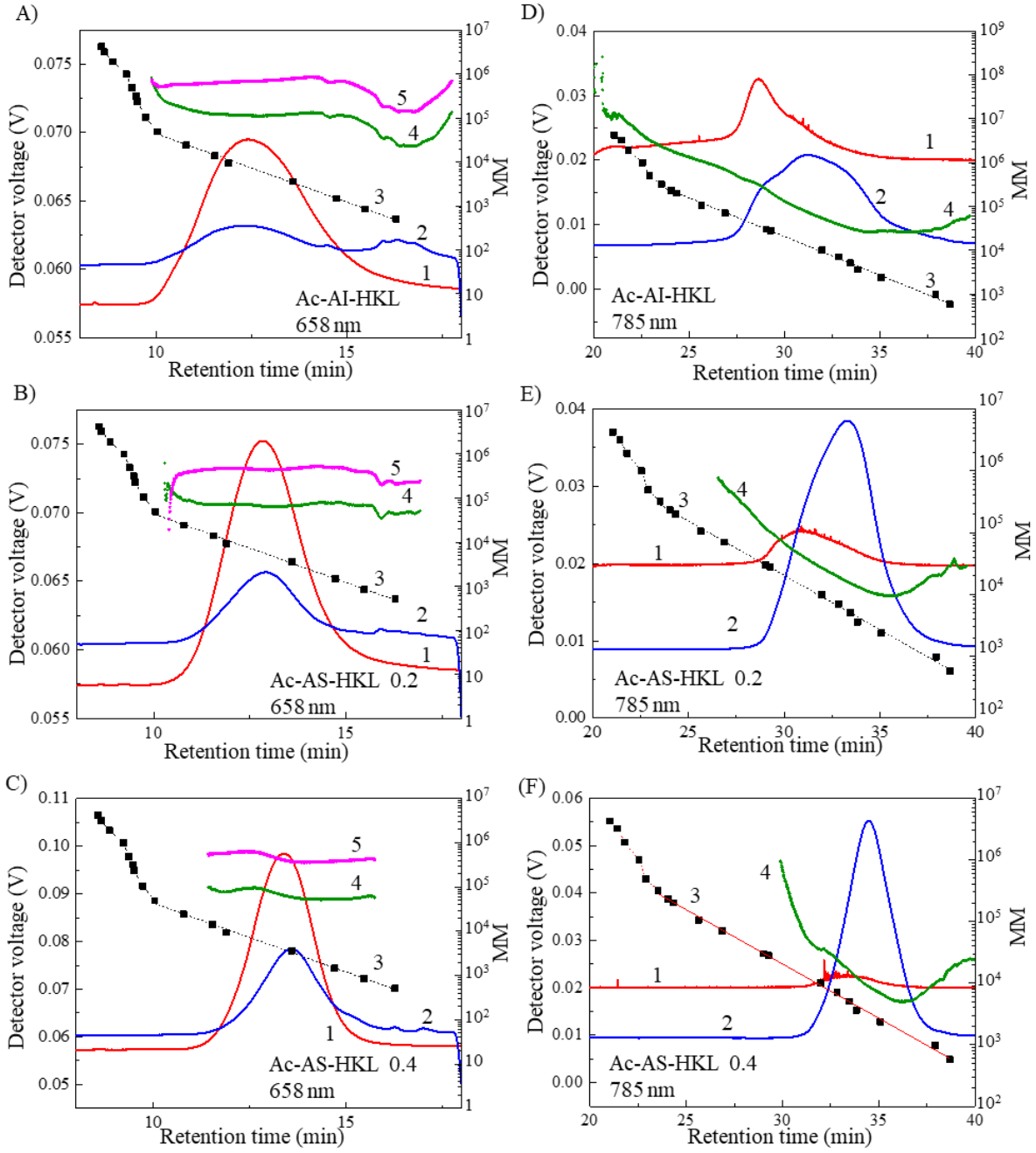

Figure 2-4. SEC-MALS-RI chromatograms of (A) Ac-AI-HKL, (B) Ac-AS-HKL 0.2, (C) Ac-AS-HKL 0.4 obtained at 658 nm, and (D) Ac-AI-HKL, (E) Ac-AS-HKL 0.2, (F) Ac-AS-HKL 0.4 obtained at 785 nm.

As shown in Figure 2-3-A), when using the MALS detector at a laser wavelength of 658 nm, the absolute MM estimated using the unfiltered photodiode was approximately 10 times larger than that estimated using the filtered one. This result strongly suggested the effect of

lignin self-fluorescence on MM when band filters were not used. The self-fluorescence of lignin significantly affected the MALS response and resulted in an overestimation of absolute MM at 658 nm. Furthermore, absolute MM curves in both plots were flat, and no relationship was observed between the MM and retention time. This relationship contradicted the principle of the SEC method. Thus, MALS with a 658 nm laser is not suitable for measuring the absolute MM of Ac-HKL probably due to the influence of sample fluorescence on the MM measurement, even though the band filters were used to eliminate self-fluorescence as much as possible.

On the other hand, when using MALS with laser light of 785 nm, in which band filters were placed on all photodiodes, the absolute MM value almost linearly decreased with an increase in retention time up to 36 min, and then the MM value increased. This result suggested that this MALS technique can be used to obtain the correct absolute MM value until 36 min. After 36 min, the absolute MM value may be incorrect because MM of small molecules could not be measured with the light-scattering method due to their small scattering intensity. The SEC-MALS chromatograms of Ac-HKL fractions in Figure 2-4 show the same result. Therefore, MALS with a 785 nm laser is suitable for measuring the absolute MM of HKL.

2.3.4. MM and $Đ_M$ of HKL and its fractions

Table 1 shows Mn, Mw and $Đ_M$ of HKL and its fractions obtained by SEC-MALS with a 785 nm laser and SEC-RI with a conventional polystyrene calibration curve. In both methods, the Mn and Mw values were calculated from 24 min (void volume of the used column: 233,000 g mol^{-1} of polystyrene) to 36 min (corresponding to 1700 g mol^{-1} of polystyrene).

Table 2-1. MM and $Đ_M$ values determined by SEC-MALS [a]

		HKL	AI-HKL	AS-HKL 0.2	AS-HKL-0.4
	dn/dC	0.160	0.136	0.165	0.182
Wavelength 785.3 nm (with filters)	**Mp**	27.8×10^3	77.9×10^3	16.6×10^3	7.5×10^3
	Mn	31.7×10^3	59.5×10^3	18.9×10^3	8.2×10^3
	Mw	55.5×10^3	135.1×10^3	29.7×10^3	12.5×10^3
	$Đ_M$	1.75	2.27	1.57	1.52
Relative MM referenced to polystyrene	**Mp**	4.8×10^3	10.3×10^3	4.4×10^3	2.7×10^3
	Mn	5.1×10^3	6.9×10^3	4.7×10^3	3.0×10^3
	Mw	8.5×10^3	13.6×10^3	7.1×10^3	3.4×10^3
	$Đ_M$	1.68	1.98	1.49	1.14

Mn and Mw were calculated from 24 min (233,000 g mol^{-1} of polystyrene) to 36 min (1700 g mol^{-1} of polystyrene).

[a] Mp is the MM at the highest peak of the RI chromatogram. A unit of MM is g mol^{-1}.

Comparing the Mn and Mw of HKL and its fractions (AI-HKL, AS-HKL 0.2 and AS-HKL 0.4) estimated from both SEC methods, these values of the samples calculated from SEC-MALS were much larger than those from SEC-RI. For example, the Mn and Mw of HKL obtained with SEC-MALS were approximately 6.2 and 6.5 times larger than those obtained with SEC-RI, respectively. Therefore, a general SEC measurement of lignin with a conventional calibration curve underestimates Mn and Mw.

Table 1 shows that $Đ_M$ (Mw/Mn) of all the samples calculated from SEC-MALS was slightly larger than that from SEC-RI. This reflected a larger MM of SEC-MALS than that of SEC-RI at early retention time region. For example, the MM values of Ac-HKL at 24-min from SEC-MALS and SEC-RI were 3.7×10^6 and 2.4×10^5 g mol^{-1}, respectively, which corresponds to a 15.4 ratio. This ratio of 36 min is 10.6. Thus, the Mw of HKL obtained from SEC-MALS was much larger than that from SEC-RI, and the difference in Mw values greatly affects $Đ_M$.

Here, $Đ_M$ of the larger MM fraction, AI-HKL, is discussed. This fraction lacked small molecules in HKL, which is removed by the solvent precipitation. The $Đ_M$ of AI-HKL calculated from both methods was larger than $Đ_M$ of HKL. Figure 2-1 shows that the RI response of AI-HKL was clearly observed at an earlier retention time, i.e., from 24-27 min, than that of HKL. The larger MM of AI-HKL was more pronounced to a big $Đ_M$.

The above MM of HKL and its fractions calculated from 24 min to 36 min might be overestimated, as the calculation ignored the small molecules eluted after 36 min. To solve this problem, linear fitting of the absolute MM was created based on the linear part of blue solid line for each MM curve from MALS, as shown in Figure 2-5, and the line was extrapolated from 23.6 min to 39.3 min, which were corresponded to polystyrenes with MM of 300,000 g mol^{-1} and 500 g mol^{-1}, respectively. Thereby, this revised MM curve covered all eluted molecules. The MM and $Đ_M$ obtained from revised MM curve and conventional calibration curve were listed in Table 2-2. Both Mn and Mw obtained from linear fitting curve (23.6 to 39.3 min) were smaller than those obtained from the previous MM curve (24 to 36 min). In the case of HKL and its fractions, the Mn and Mw were 50-90% and 80-90% of the previous values, respectively. It is convinced that Mn and Mw from linear fitting is more accurate than the previous calculation with narrow retention time.

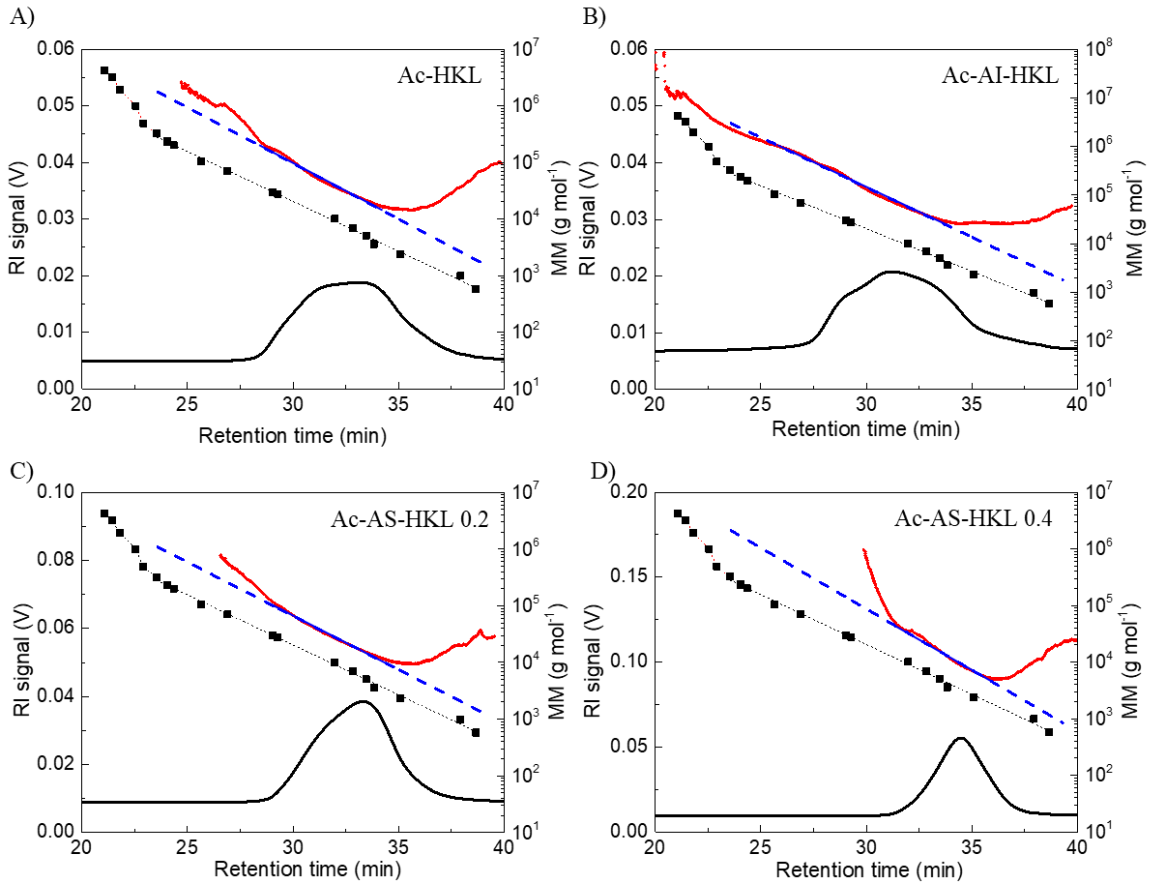

Figure 2-5. Linear fitting of MM curve for A) Ac-HKL, B) Ac-AI-HKL, C) Ac-AS-HKL 0.2 and D) Ac-AS-HKL 0.4. The red solid line was the original MM curve obtained by SEC-MALS; the blue dashed line was the linear fitting curve; the line with black square was the conventional calibration curve made from authentic polystyrene.

Table 2-2. MM and $Đ_M$ values determined by SEC-MALS after linear fitting at the retention range from 23.6 min to 39.3 min.

		HKL	AI-HKL	AS-HKL 0.2	AS-HKL-0.4
Wavelength 785.3 nm (with filters)	**Mp**	23.6×10^3	81.3×10^3	15.7×10^3	9.4×10^3
	Mn	16.1×10^3	31.5×10^3	13.1×10^3	7.3×10^3
	Mw	42.1×10^3	113.3×10^3	24.8×10^3	11.0×10^3
	$Đ_M$	2.61	3.60	1.89	1.49
Relative MM referenced to polystyrene	**Mp**	4.8×10^3	10.3×10^3	4.4×10^3	2.7×10^3
	Mn	3.5×10^3	4.9×10^3	3.8×10^3	2.3×10^3
	Mw	7.8×10^3	13.0×10^3	6.6×10^3	3.0×10^3
	$Đ_M$	2.21	2.65	1.75	1.29

Mn and Mw were calculated from 23.6 min (300,000 g mol^{-1} of polystyrene) to 39.3 min (500 g mol^{-1} of polystyrene).

[a] Mp is the MM at the highest peak of the RI chromatogram. A unit of MM is g mol^{-1}.

2.3.5. Establishment of the parameters, k and a, in Mark-Houwink-Sakurada equation for HKL

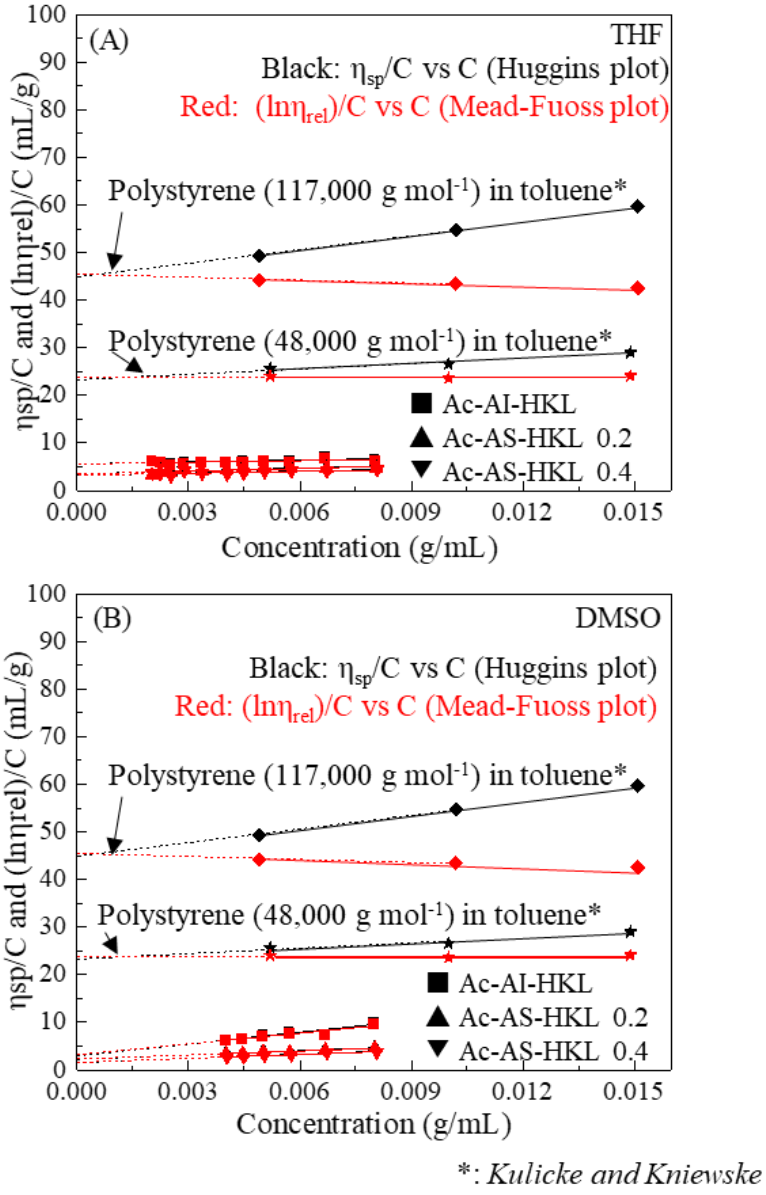

Figure 2-6. Huggins plots and Mead-Fuoss plots for acetylated HKL fractions in (A) THF and (B) DMSO solvent.

A viscosity measurement is an easy method to determine MM of a polymer, because expensive and special apparatuses are not required. However, parameters “a” and “K” in Mark-

Houwink-Sakurada (MHS) equation ($[\eta] = KM^a$, where $[\eta]$ is intrinsic viscosity, and M is MM of specimen) should be established before measurement. In this study, the MHS for Ac-HKL was established based on Mw of Ac-HKL and its fractions obtained by SEC-MALS.

MHS equation is transformed into $\log [\eta] = \log K + a \cdot \log M$. Thereby, parameters "a" and "K" are easy calculated by plotting of $\log[\eta]$ against logM. $[\eta]$, which is equal to $\lim_{c\to 0} \frac{\eta_{sp}}{c}$ or $\lim_{c\to 0} \frac{\ln \eta_{rel}}{c}$, is determined by using Huggins plot (η_{sp}/C vs. C, $\eta_{sp}/C = [\eta] + k'[\eta]^2C$) and Mead-Fuoss plot ($(\ln \eta_{rel})/C$ vs. C, $(\ln \eta_{rel})/C = [\eta] + (k'-0.5)[\eta]^2C$), where k' is Huggins coefficient and usually in the range of 0.35-0.40 for polymers (Flory 1953). Therefore, Huggins plot shows the positive slope, and Mead-Fuoss plots shows the negative plots. The slopes in both plots results from the interaction of polymer molecules with each other. When no interaction between polymer molecules like Einstein's sphere, both plots gives a horizontal line. Authentic polystyrenes (Mn of 48000 g mol^{-1} and 117000 g mol^{-1}; $Đ_M$ of 1.05) displayed typical both plots with slope, as shown in Figure 2-6, which were made from literature values (Kulicke and Kniewske 1984).

By contrast, both plots for HKL fractions with different Mw (135,100 g mol^{-1} for AI-HKL, 29,700 g mol^{-1} for AS-HKL 0.2 and 12,500 g mol^{-1} for AS-HKL 0.4) were almost horizontal (no slope) and overlapped, indicating no interaction between HKL molecules. Consequently, HKL molecules behaved like Einstein's sphere. This means HKL has very compact solution structure.

According to the compact structure, $[\eta]$ of AI-HKL (Mn = 59,500 g mol^{-1}and Mw = 135,000 g mol^{-1}) was much lower than that of polystyrene (Mn ≈ Mw = 48,000 g mol^{-1}), although Mn and Mw of AI-HKL were larger than those of polystyrene.

[η] values for three HKL fraction are listed in Table 2-2. Parameter "a" and "K" in MHS equation was obtained from the values by using the logarithm plot as shown in Figure 2-7. Finally, MHS equation for Ac-HKL was established as follows: $[\eta]/\text{mL g}^{-1} = 0.320\ M^{0.24}$ (R^2 = 0.949) in THF and $[\eta]/\text{mL g}^{-1} = 0.142\ M^{0.26}$ ($R^2 = 0.950$) in DMSO. The exponent "a" values of HKL in THF and DMSO were in the range of 0.12-0.32, which agreed with those reported in the 1960s and 1970s for several isolated lignins in aqueous alkaline solutions and organic solvents (Goring 1971). The exponent "a" for Ac-HKL in both THF and DMSO were much smaller than that of a compact coil (a=0.5), instead the value was close to that of Einstein's sphere (a=0), suggesting that the HKL molecule likely has a similar shape to that of Einstein's sphere. In addition, the exponent "a" in THF was remarkably smaller than the value of 0.725 for polystyrene in THF(Alliet and Pacco 1968; Spatorico and Coulter 1973) The low "a" also clearly revealed that the conformation of the HKL molecule was more compact than that of polystyrene. The compact conformation of HKL explains why the Mw and Mn values of HKL calculated from the SEC-RI results were much smaller than those from the SEC-MALS results.

Table 2-2. Intrinsic viscosity of the HKL fractions in THF and DMSO

	AI-HKL	**AS-HKL 0.2**	**AS-HKL-0.4**
$[\eta]_{THF}$ **(mL g^{-1})**	5.60	3.50	3.23
$[\eta]_{DMSO}$ **(mL g^{-1})**	2.98	2.24	1.57

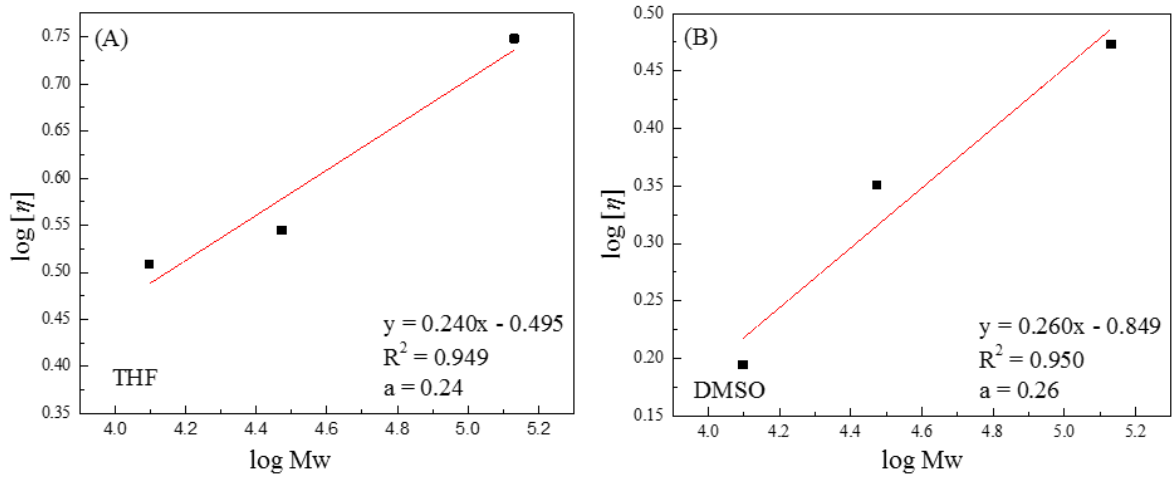

Figure 2-7. Logarithmic plot of [η] versus the absolute Mw for HKL fractions in (A) THF and (B) DMSO

2.4. Conclusion

The MMs of acetylated HKL and its fractions were obtained by two SEC-MALS systems at the wavelengths of 658 nm and 785 nm. As the chromatogram obtained from SEC-MALS at 658 nm did not obey the SEC theory, the laser light at 658 nm was found to be unsuitable for lignin MM determination. In this system, lignin self-fluorescence could not be eliminated even though the band filter was equipped. On the other hand, the SEC-MALS system with a laser light of 785 nm and a band filter clearly demonstrated a retention time dependency of MM, suggesting that this system enables to measure a more accurate absolute MM of HKL.

The Mw and Mn of Ac-HKL calculated from the SEC-MALS data were much larger than those calculated from the SEC-RI data. This phenomenon was attributed to the compact solution structure of the HKL molecule in THF. The low exponent "a" value in the Mark-Houwink-Sakurada equation for HKL in THF ($[\eta]$/mL g^{-1} = 0.320 $M^{0.24}$) also indicates a compact solution structure of lignin.

Chapter 3. Relationships between MM of lignin and its branched structure

3.1. Introduction

In the last chapter, HKL was confirmed to have a compact solution structure, which resulted in a larger absolute MM compared to the relative MM at any given hydrodynamic radius or retention time of SEC. A hypothesis was proposed that such compact structure of lignin might be caused from branched structure of lignin. According to the study reported by Lyulin et al.(Lyulin et al. 2001), the polymer with many branching points has a more compact structure in solution. Lue also reported that a dendritic polymer has a more compact structure in solution than that of a linear polymer with an identical MM (Lue 2000).

To verify the hypothesis, in this chapter, the SEC-MALS analysis of acetylated 8-O-4' type of linear polymeric lignin model (Ac-M-8O4') in addition to softwood and hardwood kraft lignins is conducted to compare the swelling behavior between kraft lignins and the linear lignin model. This lignin model is comprised of only an 8-O-4' interunitary linkage, which was a predominant linkage in the native lignin. Thereby, this can be considered to be the most suitable compound as a reference of linear polymer for investigating effect of the branched structure of isolated lignin on swelling behavior of lignin.

Among the interunitary linkages of lignin, 5-5' and 4-O-5' are proposed to be branching points. Chang and Jiang well reviewed the frequencies of such linkages, as shown in Table 3-1 (Chang and Jiang 2020). Although their frequencies vary dependent on the wood species and determination methods, the frequency (19–27%,) of 5-5' linkage (Bose et al. 1998; Capanema et al. 2004; Pew 1963) is much larger than the 4-O-5' frequency (3.5-4%) (Erickson et al. 1973).

In this study, the frequency of the 5-5’ linkage in kraft lignins was determined by a combinational method of alkaline nitrobenzene oxidation and 1H-NMR. From the results, the relationship between lignin MM and branching frequency is discussed.

Table 3-1. Linkage frequency of 5-5’ and 4-*O*-5’.

	Frequency (per 100 C9)	Wood species	Determination method	Ref.
5-5’	25	Spruce	UV spectral method	Pew 1963
	19-22	Spruce	CuO/NaOH-Permanganate oxidation	Erickson et al. 1973
	24-26	Spruce	13C NMR	Drumond et al. 1989
	24-27	Spruce	2D HSQC NMR	Capanema et al. 2004
4-*O*-5’	4	Spruce	CuO/NaOH-Permanganate oxidation	Erickson et al. 1973
	1	Pine	2D HSQC NMR	Yue et al. 2016

3.2. Experimental

3.2.1. Sample preparation for the SEC-MALS analysis

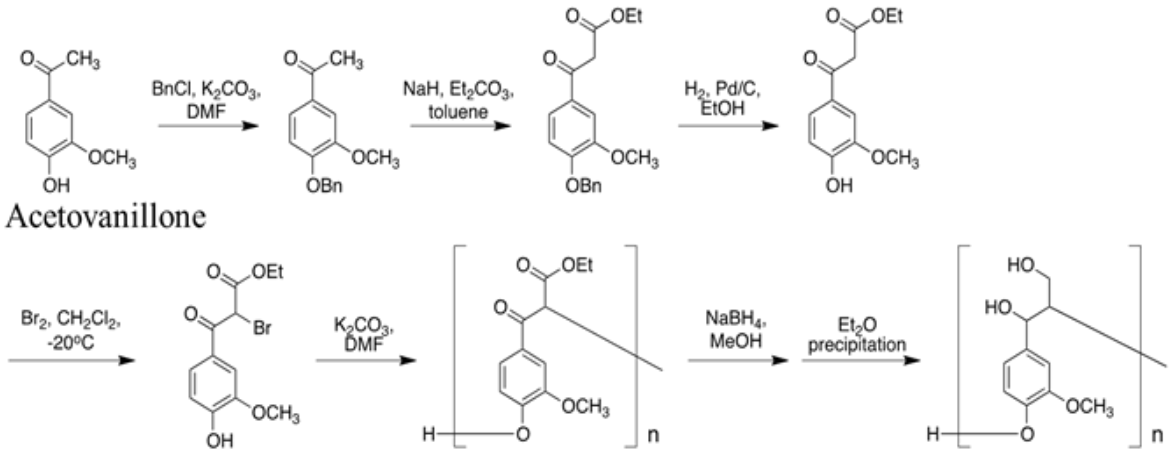

Figure 3-1. Synthesis of M-8O4’ (Bn = -CH_2-C_6H_5, Et = -CH_2-CH_3)

Hardwood kraft lignin (HKL) and softwood kraft lignin (SKL) were precipitated by acidification of kraft pulping black liquors of Eucalyptus *exserta F.Muell* (supplied from Hainan Jinhai Pulp Paper Co., Ltd., Danzhou, China) and of a mixture of several Hokkaido coniferous woods (supplied from Oji Paper Co., Ltd., Tomakomai, Japan), respectively. The precipitates were collected by filtration and washed with distilled water until pH 3. The resultant precipitates were dried in air, and then *in vacuo* at 50°C for 48 h to obtain HKL and SKL powders. A *8-O-4'* type polymeric lignin model (M-8O4') was supplied by Dr. K. Shigetomi (Hokkaido University, Japan), which was prepared according to previous reports (Kishimoto et al. 2006 2008a 2008b). This synthetic route is simply shown in Figure 3-1. The HKL, SKL and M-8O4' powders (500 mg) were acetylated with 10 mL acetic anhydride-pyridine (1:1, v/v) at room temperature for 48 h. The acetylated samples were precipitated by pouring the mixture into distilled water with ice, and the precipitates were collected by centrifugation. The precipitates were further washed with distilled water followed by lyophilization to yield Ac-HKL, Ac-SKL and Ac-M-8O4'.

3.2.2. MALDI-TOF MS measurement

A MALDI-TOF MS measurement was performed on an Applied Biosystems Voyager DE-STR instrument (CA, USA) operating in a positive-ion linear mode with a pulsed UV laser beam (nitrogen laser, A=337 nm). An accelerating voltage was 20 kV. M-8O4' was first dissolved in acetone-water (9:1, v/v) at 0.1 mg mL^{-1}, and 1.5 μL of the sample solution was dropped to the target plate. Then the same amount of the matrix solution containing 20 mg mL^{-}

[1] of 2,5-dihydroxybenzoic acid and 4.2 mg mL^{-1} of LiCl in Milli-Q water was added to the plate. The measurement was performed after the removal of solvent by air flow.

3.2.3. Determination of MM by SEC-MALS

Specific refractive index increments (*dn*/*dc*) of all lignin samples for MM calculation were determined on an automatic refractometer (Abbemat 550, Anton Paar, Graz, Austria), which was different from the refractometer using in Chapter 2. The wavelength of the polarized light was 589 nm. Sample solutions at different concentrations were placed on the cell of the refractometer at 25°C. The *dn*/*dc* values were calculated from the tangent for the plot of the refractive index against concentration.

SEC-MALS measurements were conducted under the same conditions and procedure as mentioned in Chapter 2. The MALS detector was equipped with 785 nm laser light and bandpass filters.

3.2.4. Calculation of hydrodynamic radius for Ac-HKL, Ac-SKL and Ac-M-8O4'

Hydrodynamic radius, "*r*", is expressed as $[\eta]M = 2.5N_A V_e = 2.5N_A \cdot \frac{4}{3}\pi r^3$ (Sperling 2005), which is derived from Einstein equation $[\eta = \eta_0(1+2.5v_2)]$. How to get $[\eta]M$ as a function of "r" is described in Equation 3-1 to 3-6 at the end of this section. To estimate "r" at each retention time of SEC, $[\eta]M$ was obtained from a universal calibration curve "log$[\eta]M$ vs. retention time" of authentic polystyrene (Grubisic et al. 1967), where $[\eta]$ and M of authentic polystyrenes were cited from the website of American Polymer Standards Corporation

(http://www.ampolymer.com/Standards/Polystyrene.html).

The universal calibration curve of authentic polystyrenes in THF is shown in Figure 3-2. When "r" of polystyrene with Mn of 2,350 g mol^{-1} at the retention time of 35 min is estimated, $[\eta]M$ of 90.2 dL mol^{-1} is inserted into Eq 3-6. As a result, "r" at 35 min is 1.2 nm. This "r" value can be applied to any polymer including Ac-HKL, Ac-SKL and Ac-M-8O4'.

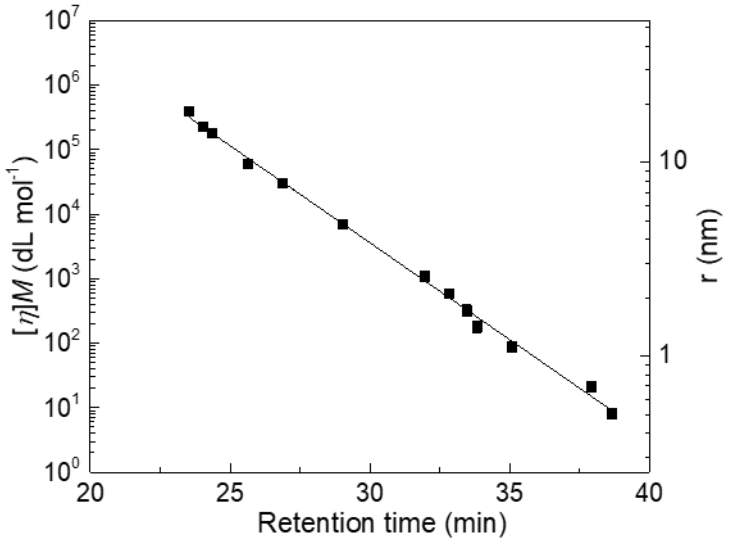

Figure 3-2. Universal calibration curve of polystyrene standards. Left Y-axis shows the values of log $[\eta]M$, and right Y-axis shows the hydrodynamic radius.

$\eta = \eta_0(1+2.5v_2)$ Einstein equation (3-1)

$$\frac{\eta-\eta_0}{\eta_0} = \eta_{sp} = 2.5\, v_2 = 2.5\left(\frac{n_2}{V}\right)V_e \quad (3\text{-}2)$$

$$\frac{n_2}{V} = \frac{cN_A}{M} \quad (3\text{-}3)$$

$$\left[\frac{\eta_{sp}}{c}\right]_{c=0} = [\eta] = 2.5\frac{N_A V_e}{M} \quad (3\text{-}4)$$

$$[\eta]M = 2.5N_A V_e = 2.5N_A \cdot \frac{4}{3}\pi r^3 \quad (3\text{-}5)$$

$$r = \sqrt[3]{\frac{3}{4} \times \frac{[\eta]M}{2.5\pi N_A}} \quad (3\text{-}6)$$

where η is the viscosity of solution, η_0 is the viscosity of solvent, η_{sp} is the specific viscosity, v_2 is the volume fraction of spheres, n_2/V is the number of molecules per unit volume, V_e is the equivalent volume of the spherical molecule, c is the concentration and N_A is Avogadro's number.

3.2.5. Quantification of the 5-5' interunit linkage of lignins and their fractions

Kraft lignin fractions were prepared according to previous reports (Cui et al. 2014; Wang et al. 2019), as mentioned in Chapter 2. As a first process of this quantification, the specimens were subjected to the alkaline nitrobenzene oxidation. A scheme of this process is shown in Figure 3-3. Twenty-five milligram of each sample was reacted with 0.24 mL of nitrobenzene and 4 mL of a 2 M NaOH aqueous solution in a 20-mL stainless steel vessel for 2 h at 170°C in an oil bath. The reaction vessel was cooled to room temperature by its immersion in running water. Then, 0.5 mL of 1,4-dioxane containing 2.5 mg of 5-iodovanillin as an internal standard was added to the reaction mixture. The mixture was filtered, and the residue was washed with 0.2 M NaOH (1 mL×3). The filtrate and washings were combined and acidified to pH 2–3 with a 0.5 M HCl solution. Then, the solution was extracted with ethyl acetate (30 mL×3), and the organic layer was washed with brine and dried over Na_2SO_4. The products were acetylated with 2 mL of acetic anhydride/pyridine (1:1, v/v) at 50°C for 2 h. After removing the acetylating reagents by evaporation with toluene, the acetylated products were dried *in vacuo* at room

temperature. The resultant sample was dissolved in chloroform-*d* with tetramethylsilane as an internal standard and analyzed with a 270 MHz-^{1}H-NMR (JNM-EX270, JEOL, Tokyo, Japan). Aldehyde signals of each products at 9.86 ppm, 9.90ppm, 9.94 ppm and 9.95 ppm were quantified from the signal area after the deconvolution of the overlapping signals with MestReNova software.

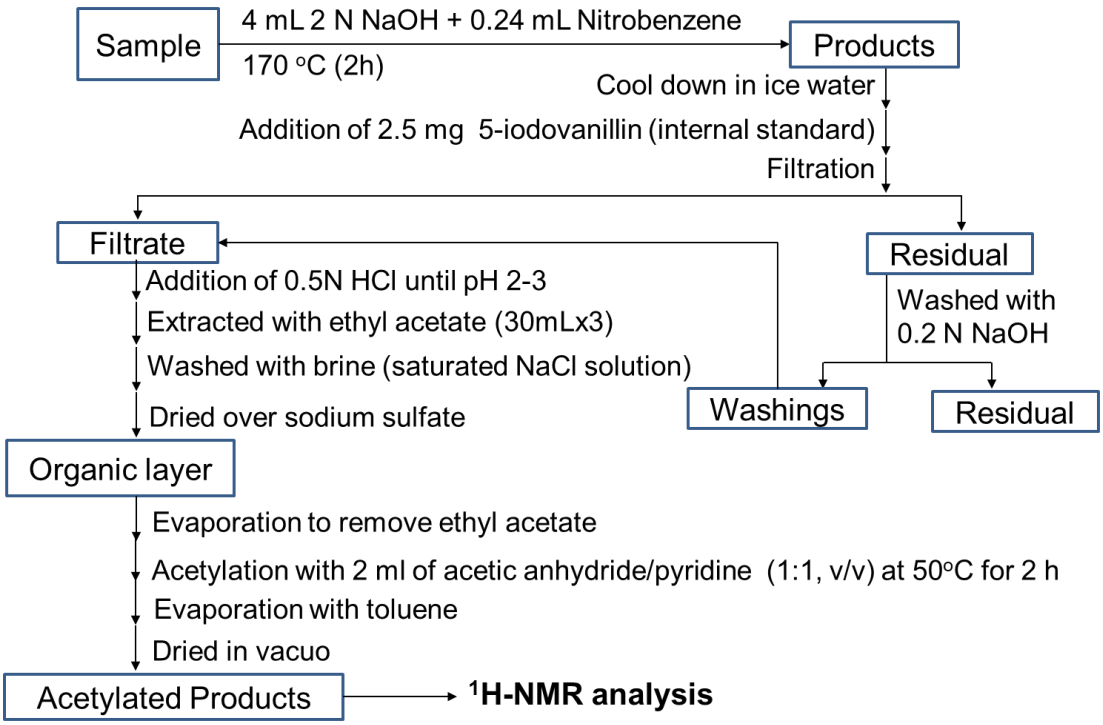

Figure 3-3. 5-5' structure determined by alkaline nitrobenzene oxidation

3.3. Results and discussion

3.3.1. SEC-MALS measurement of three acetylated lignin samples

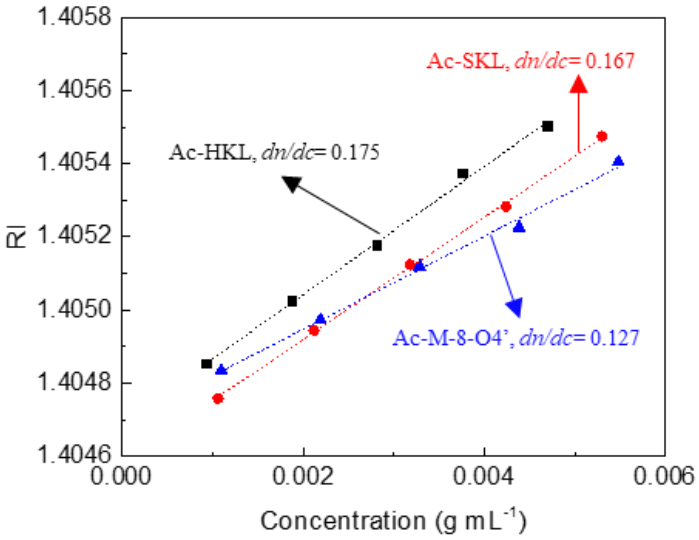

Figure 3-4. Refractive indices of Ac-HKL, Ac-SKL and Ac-M-8O4'.

Figure 3-4 shows the RI values versus concentration of Ac-SKL, Ac-HKL and Ac-M-8O4'. From the slope of these lines, *dn*/*dC* values were calculated to be 0.175 mL g^{-1} for Ac-HKL, 0.167 mL g^{-1} for Ac-SKL and 0.127 mL g^{-1} for Ac-M-8O4'. These values were further used for SEC-MALS analysis.

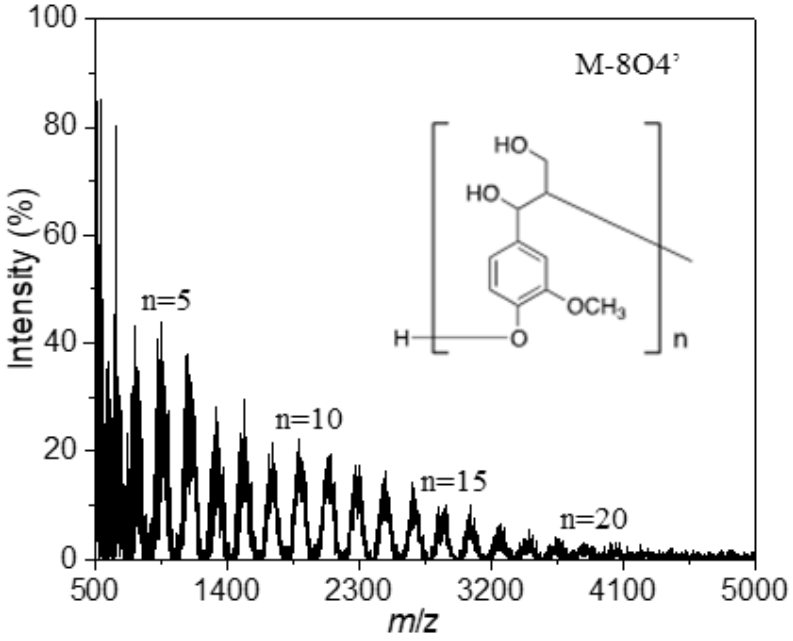

Figure 3-5. MALDI-TOF mass spectrum of M-8O4'

Figure 3-5 shows the structure of a *8-O-4'* type linear polymeric lignin model (M-8O4') and its MALDI-TOF mass spectrum. The molecular ion peaks were observed at intervals of m/z 196, which was corresponded to the mass of the repeating unit. However, the signal intensities were decreased with the increase in degree of polymerization (DP), and the signal was hardly observed at DP > 20, i.e. MM > 4,000 g mol^{-1}, which indicated that M-8O4' is like an oligomer compound with relatively low MM. This result was later compared with the SEC-MALS analysis.

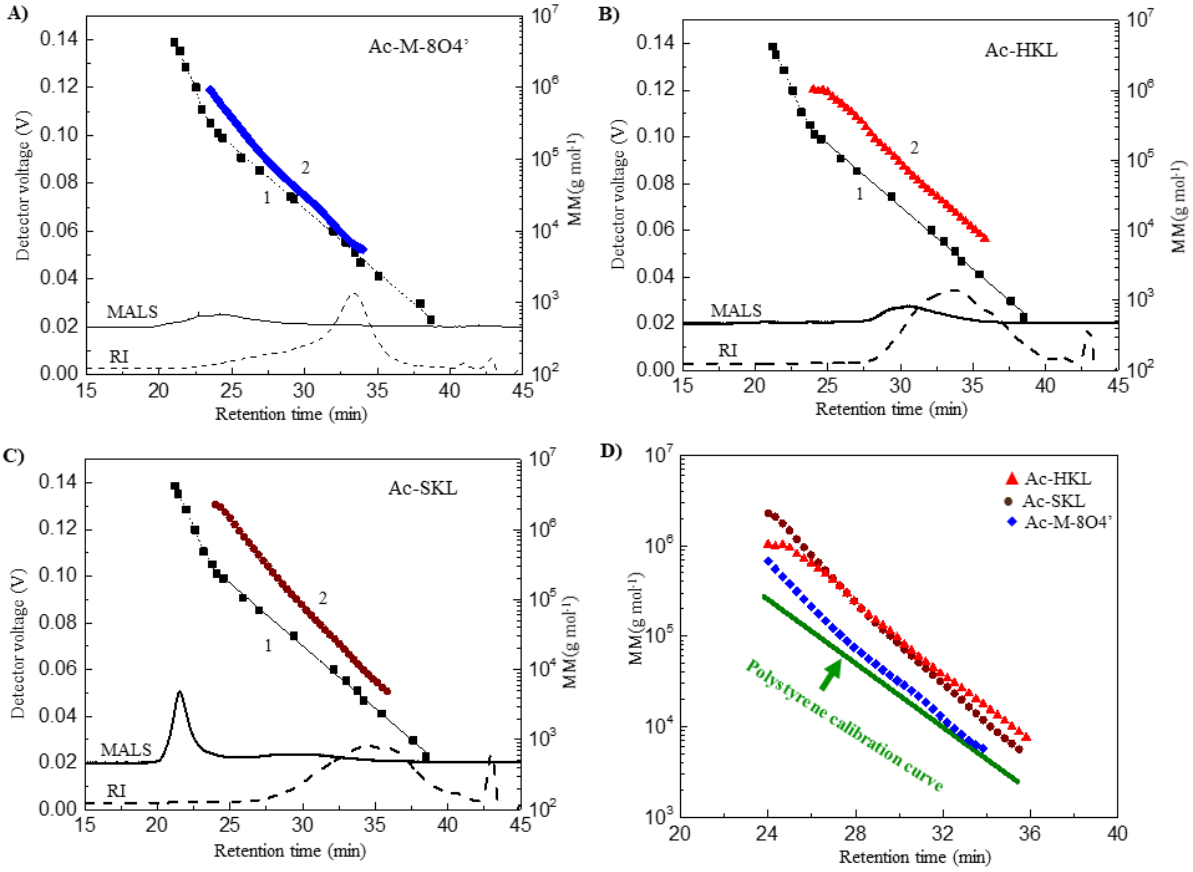

Figure 3-6. SEC-MALS-RI chromatograms:A), Ac-M-8O4'; B), Ac-HKL; C), Ac-SKL. D), overlaid MM curves of three lignin samples.

Figures 3-6-A, B and C show the SEC-MALS-RI profiles of acetylated M-8O4' and kraft lignins. The MM curves of Ac-M-8O4' and acetylated kraft lignins were obtained by MALS responses and RI increment (*dn*/*dc*) values. In three subfigures, the MALS signals always appeared at an earlier retention time than the RI signals, which indicates the higher sensitivity of the light scattering detector for larger MM molecules. In Figure 3-6-A, Ac-M-8O4' exhibited the peak top MM (Mp) at 6.4×10^3 g mol^{-1} in the RI chromatogram, and the RI response was observed even at the higher MM region (10^4–10^6 g mol^{-1}). This result is not consistent with that of MALDI-TOF-MS. Although MALDI-TOF-MS is a powerful technique, especially for

qualitative analysis to confirm residual MM of the repeating unit, the method does not completely cover the actual MM distribution of M-8O4', which results from the suppressed ionization of the high MM fraction compared to the low MM fraction. Thus, the conventional SEC system is still irreplaceable for the MM determination of the polymers.

As shown in Figure 3-6-A, a MM curve of Ac-M-8O4' was almost overlapped with a calibration curve created with polystyrene standards. This result shows that Ac-M-8O4' has a similar swelling behavior to that of polystyrene in THF. Therefore, the predominant 8-*O*-4' linkage in lignin does not contribute to the discrepancy between lignin MM and polystyrene MM. By contrast, the MM values of acetylated softwood kraft lignin (Ac-SKL) and hardwood kraft lignin (Ac-HKL) were approximately 5- to 10-fold larger than the MM value of polystyrene at any retention time (Figures 3-6-B and C), which shows distinctly different swelling behaviors; Ac-KLs have more compact structure than those of linear polymers, such as polystyrene and the polymeric lignin model. This tendency was also observed for the relationship between underivatized lignins and polystyrene sulfonates in LiBr/DMSO (Zinovyev et al. 2018). Although the results from different solvent systems are not directly compared, it can be speculated that the compact morphology of kraft lignins is not attributed to the free hydroxy group, which enables to form the intramolecular hydrogen bonds. To better compare the MM of these three lignin samples, MM vs. retention time curves were overlaid in Figure 3-6-D. Figure 3-6-D displays a similar swelling behavior of Ac-SKL and Ac-HKL. Of course, the swelling behavior is quite different from those of the linear compounds. This result also indicates that the swelling behavior of acetylated lignins is independent of monomeric compositions (i.e. guaiacyl (G)/syringyl (S) ratio). Overall, these observations imply the

involvement of other structural features in compact morphologies of kraft lignins. Next, the effect of branched substructure on kraft lignin morphology is investigated.

3.3.2. Determination of the frequency of 5-5' linkage in lignins and their fractions

Alkaline nitrobenzene oxidation can provide a biphenyl product derived from the 5-5' substructure in addition to G- and S-types of monomeric products, and the product allows to estimate the frequency of the 5-5' substructure in the original sample by combining ^{1}H-NMR spectroscopy (Katahira and Nakatsubo 2001). The formyl proton signals of acetylated nitrobenzene oxidation products from M-8O4', SKL and HKL are shown in Figure 3-7-A. The signals at 9.95 ppm, 9.94 ppm and 9.90 ppm can be assigned to the 5-5' type, G-type and S-type products, respectively. However, as the signals of 5-5' and G-types are partly overlapped, the area of the signals must be deconvoluted for quantification as shown in Figure 3-7-B. The molar contents (MC, mmol $g^{-1}$of lignin) of these products were calculated based on the area of acetylated 5-iodovanillin as an internal standard. The frequency or abundance of 5-5' interunitary linkage was calculated based on Eq.3-1

$$\text{5-5' abundance} = MC_{5\text{-}5'}/(2MC_{5\text{-}5'}+MC_G+MC_S) \times 100 \quad (3\text{-}1)$$

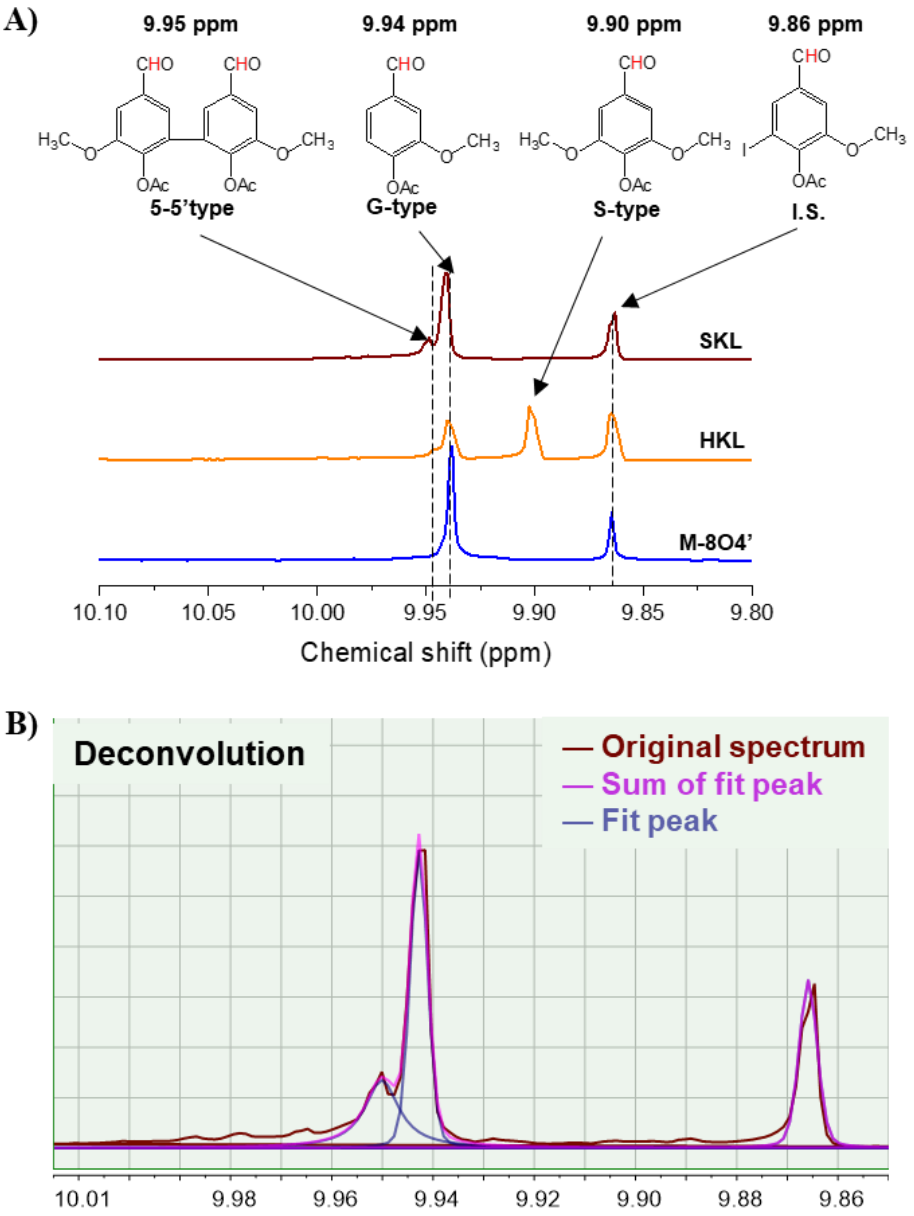

Figure 3-7. ^{1}H NMR spectrum of A) acetylated nitrobenzene oxidation products from SKL, HKL and M-8O4', and B) the deconvolution chart for SKL products

To further obtain the information on the branching frequency in lignin, the fractionated lignin samples were also subjected to the combination analysis method, where the fractionated samples of two kraft lignins were prepared by the solvent precipitation using acetone and hexane in accordance with the procedure reported by Cui et al (Cui et al. 2014). The SEC-RI

chromatogram of each acetylated fraction is shown in Figure 3-8. The chromatograms clearly demonstrate that the solvent fractionations for both SKL and HKL are successfully carried out, and provide the fractions with different Mp and narrow MM distributions. The number in parentheses shows the mass percentage of each fraction.

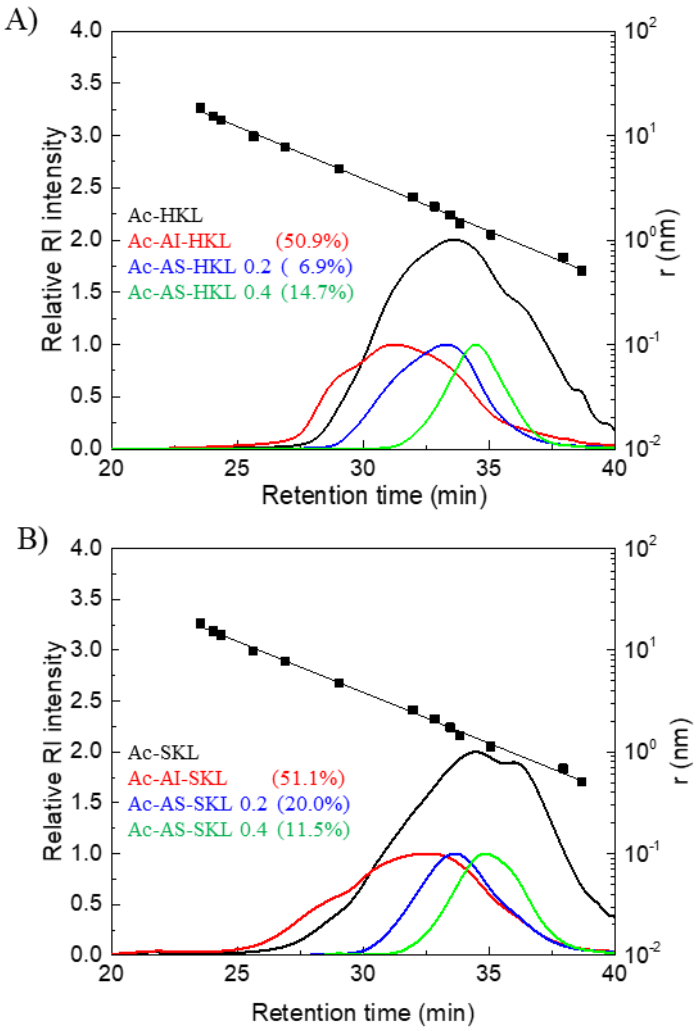

Figure 3-8. SEC-RI chromatograms of A) Ac-HKL and its fractions and B) Ac-SKL and its fractions. The solid line with black square shows the hydrodynamic radius at each retention time.

Table 3-2 summarizes the quantitative results of 5-5’ frequency as well as monomeric products of alkaline nitrobenzene oxidation. In all fractions, SKLs showed a higher 5-5’ abundance than those of HKLs. This result well reflects the predominance of the guaiacyl unit in original coniferous lignin, in which the C5 position is unsubstituted and involves the condensation of two aromatic rings. These two unoccupied positions easily form the 5-5’ bonds during lignin biosynthesis process. When focusing on different fractions, the 5-5’ abundances of AI-SKL and AI-HKL (20.0 and 12.3 per 100 Ar, respectively) are higher than those of corresponding unfractionated kraft lignins and acetone-soluble fractions. In addition, no significant difference in 5-5’ abundance between AS-SKL0.2 and AS-SKL0.4 was observed (15.2 and 16.2 per 100 Ar, respectively) regardless of their different MM distributions; similarly, no significant difference in 5-5’ abundance between AS-HKL0.2 and AS-HKL0.4 was observed (8.2 and 7.1 per 100 Ar, respectively). Crestini et al.(Crestini et al. 2017) reported that the AI-KL fraction retained the frequencies of 8-*O*-4’, 8-5’ and 8-8’ linkages in native lignin, while AS-KLs as smaller MM fractions were severely degraded by kraft cooking. Dramatic structural changes of AS-KLs were confirmed by their increased phenolic hydroxy group, a decrease hydrogen atom in aromatic ring (C-H), and the loss of aliphatic sidechain. The proposed reactions are shown in Figure 3-8. The phenolic lignin unit transformed into quinone methide under alkaline condition, and then undergone retro-aldol reaction to produce phenolic compound with the removal of aliphatic side chain, as shown in Figure 3-9-A. The resultant phenolic compound was supposed to undergo radical repolymerization to form the final compounds with less aliphatic sidechains and more substituted groups in aromatic ring, as shown in Figure 3-9-B. The less aliphatic side chains and more substituted aromatic rings

explained the lowered 5-5’ abundances in AS-KLs when nitrobenzene oxidation was applied as the determination method.

Table 3-2. 5-5’ abundance of kraft lignins and their fractions

	5-5’	G	S	5-5’ abundance
		(mmol g^{-1})		(per 100 Ar)
M-8O4’	-	0.519	-	0.0
Softwood KL				
SKL	0.071	0.262	-	17.4
AI-SKL	0.047	0.141	-	20.0
AS-SKL 0.2	0.100	0.457	-	15.2
AS-SKL 0.4	0.069	0.288	-	16.2
Hardwood KL				
HKL	0.027	0.142	0.209	6.7
AI-HKL	0.032	0.062	0.132	12.3
AS-HKL 0.2	0.041	0.160	0.259	8.2
AS-HKL 0.4	0.019	0.085	0.147	7.1

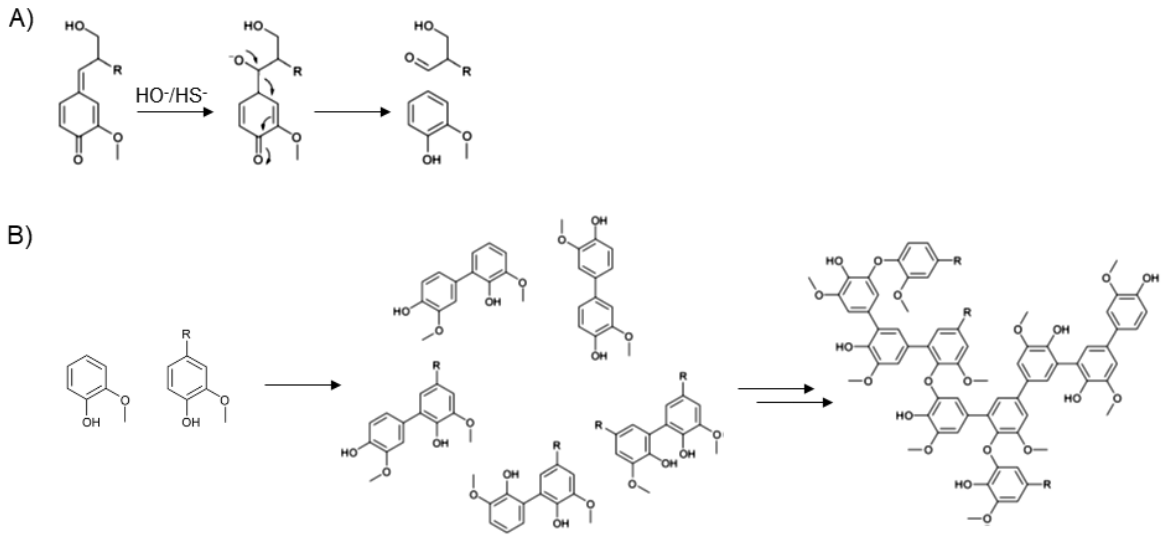

Figure 3-9. (A) C1–Cα cleavage of the lignin backbone by the retroaldol reaction and the formation of phenolic monomers. (B) Possible products arising from the radical coupling pathway of fragments released during kraft pulping. (Ref. Crestini et al. 2017)

3.3.3. Relationship between lignin MM and 5-5' abundance

After getting the MM and 5-5' abundance of lignin fractions, their relationship was studied. As shown in Figure 3-7, the retention times of Ac-AI-KL, Ac-AS-KL20 and Ac-AI-KL40 at the peak top were approximately 31, 33 and 35 min, respectively. The MM values at these retention times were plotted versus the 5-5' abundance, and regression lines and their determination coefficients (R^2) are shown in Figure 3-10-A. The "*r*" values in the figure represent hydrodynamic radii at corresponding retention times, which were calculated from Figure 3-8. The regression lines of 33 and 31 min showed moderate to good positive correlations with the R^2 values of 0.547 and 0.737, respectively. However, there was no correlation with that of 35 min (R^2 = 0.039). The correlation of AIKL fractions at 25 min was also examined, because MALS has higher accuracy for larger molecules. The result is shown in Figure 3-9-B. Surprisingly, an excellent correlation with an R^2 value of 0.991 was obtained for these fractions. The results demonstrated that MM is proportional to the 5-5' abundance of lignin samples, and the excellent linearity is acquired for higher MM fractions. The poor correlation of the 35-min fractions may be ascribed to other branched structures (Figure 3-9-B) formed during kraft cooking which are not present in native lignins (Crestini et al. 2017). Therefore, the positive correlation between lignin MM and 5-5' abundance is caused by branched substructures in lignin molecules, resulting in less swollen, densely packed structure in solution, and this result is more valid for lignins with larger molecular sizes.

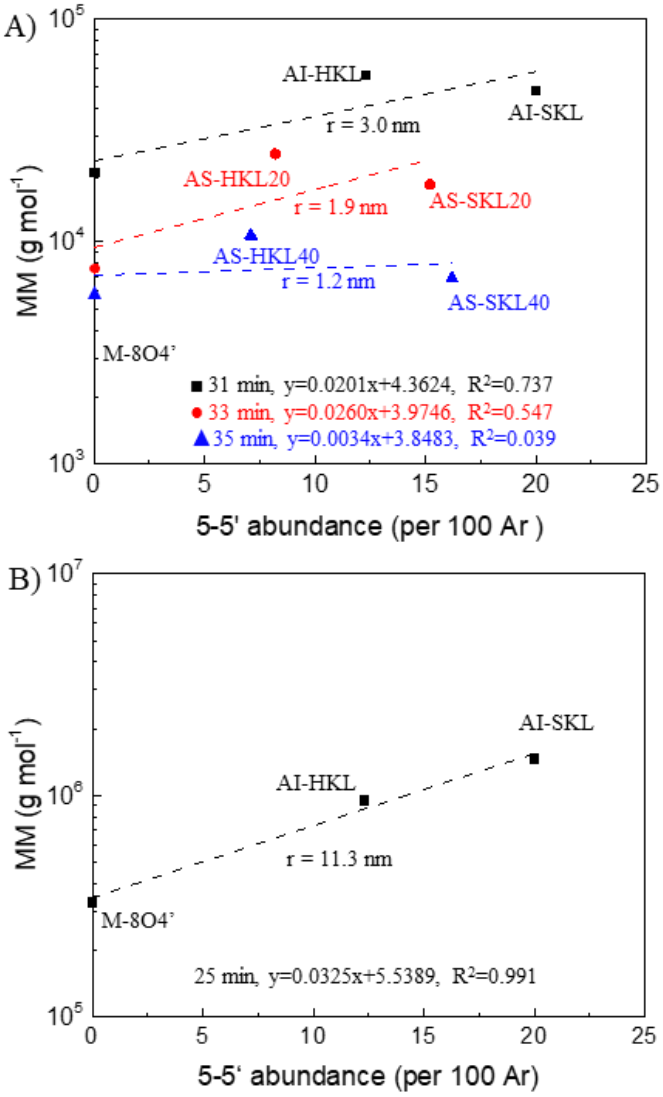

Figure 3-10. Molar mass of sample vs. the 5-5' abundance of lignin fractions at different retention times (A) and at 25 min(B). The "*r*" value shows the hydrodynamic radius of each retention time.

3.4. Conclusion

The difference in MM at any retention time of SEC between the linear lignin model and kraft lignins was clearly demonstrated by using SEC-MALS equipped with a 785 nm laser light and bandpass filters. At the same retention time, the MMs of kraft lignins were always larger

than that of the linear lignin model; thus, kraft lignin has a more compact solution structure than those of the linear 8-*O*-4' model and polystyrene.

The combination analysis of alkaline nitrobenzene oxidation and ^{1}H-NMR was used to estimate the 5-5' interunitary linkage frequency in three lignin preparations and their fractions. The relationship between the MM and 5-5' abundance was positively correlated, especially for the high MM fraction. It is clearly revealed that the more branched structure lignins have, the denser morphology lignins possess.

Chapter 4 Conclusions

4.1. Summary of this study

Molar mass (MM) determination of isolated lignins including technical lignins is one of the important subjects to elucidate their chemical structures and to further promote their industrial utilization. In 1960's, Mn and Mw of several lignins were reported to be in the digit range of 10^3-10^5 g mol^{-1} (Goring 1971). However, in the last two decades, their values were in the range of 10^3-10^4 g mol^{-1}, which were measured by using a conventional SEC method with a calibration curve created by using polystyrene. The difference in MM estimation resulted from the determination method. The conventional SEC method gives the relative Mn and Mw to the polystyrene, but not the absolute values. On the other hand, SEC-MALS enables to obtain Mn, Mw and $Đ_M$ of polymers based on the absolute MM. However, one problem of SEC-MALS for lignin MM determination is self-fluorescence of lignin, which is caused by the conjugated structures of isolated lignins and leads to the overestimation of MM.

In this study, SEC-MALS was used for lignin MM determination, and its practical conditions were investigated to minimize the self-fluorescence of lignin as much as possible. The solution structure of isolated lignins were also investigated with respect to molecular size and their branched structure. The detailed results were listed below.

1) Lignin MM obtained by SEC-MALS equipped with band filters was much smaller than that without band filters. Therefore, the band filters were effective to eliminate the self-fluorescence of lignin, resulting in an accurate lignin MM.

2) MM obtained by SEC-MALS at 658 nm did not obey the SEC theory, while MM obtained by SEC-MALS at 785 nm was reasonable because MM was decreased with the retention time. This indicated that MALS detector with longer wavelength laser light was better for lignin MM determination.

3) MM curve of Ac-M-8O4', as the linear lignin model, obtained from SEC-MALS was similar to that obtained from a conventional SEC method with a calibration curve of poltstyrene. This indicated the similarity of the solution structures between Ac-M-8O4' and linear polystyrene.

4) MM of Ac-HKL and Ac-SKL obtained from SEC-MALS was much larger than those obtained from the conventional SEC method at any retention time. This suggested that the solution structure of Ac-KLs should be more compact than that of polystyrene in THF.

5) The exponent "a" in the Mark-Howink-Sakurada equation of Ac-HKL (0.24) in THF was much smaller than that of polystyrene (0.725). This also clearly revealed that Ac-HKL had more compact solution structure than that of polystyrene.

6) The compact solution structure of kraft lignins resulted from their branched structure. Their MMs were proportional to the frequency of 5-5'interunitary linkage as branching point, especially at the early retention time or larger hydrodynamic volume region.

4.2 General discussion and outlook

This study pointed out the invalidity of the conventional SEC method for lignin MM determination, and demonstrated how to accurately measure the MM by using SEC-MALS system. Henceforth, the analyzer and analyzing protocol were proposed to measure the MM of technical lignins. This study also revealed that the branched structure caused the compact solution structure of technical lignin.

I am convinced that the findings of this research contribute to understanding not only the swelling behavior of technical lignin in a solution, but also for prediction of the reactivity of lignin functional groups for the preparation of high value-added lignin-based derivatives. So far, a derivation of technical lignins was planned based on the same reactivity of all functional groups, especially hydroxy group. However, my research predicts that the reactivity between the inside and surface functional groups should be different, because inside functional groups are hindered and inhibited to react with other reactants due to the compact solution structure of lignin. Afterwards, this prediction should be taken into consideration for the preparation of lignin derivatives.

In addition, my research achievements are also helpful to predict the structure of derivatization products coupled with other synthetic polymers. For example, the reaction of lignin with polyethylene glycol (PEG) and diisocyanate provides polyurethane, which is predicted to have phase separation or sea-island structure. The reason is that compact lignin is an island part, while flexible PEG forms a sea part. In fact, there have already been several reports on sea-island structure of lignin-based polyurethane (Cinelli et al. 2013; Saito et al. 2013; Bernardini et al. 2015). As well, the structure of resultant lignin-based derivatives

prepared by coupling with other synthetic polymers is easy to be predicted based on my research. Thus, this research is convinced to contribute to developing lignin-based value-added materials via derivatization.

References

Alliet D.F., Pacco J.M. (1968) The Investigation of Parallel-Column Systems in Gel Permeation Chromatography. *Journal of Polymer Science: Part C*. 21:199-213.

Andrianova A.A., Yeudakimenka N.A., Lilak S.L., Kozliak E.I., Ugrinov A., Sibi M.P., Kubátová A. (2018) Size Exclusion Chromatography of Lignin: the Mechanistic Aspects and Elimination of Undesired Secondary Interactions. *Journal of Chromatography a*. 1534:101-110.

Araújo J.D., Grande C.A., Rodrigues A.E. (2010) Vanillin Production From Lignin Oxidation in a Batch Reactor. *Chemical Engineering Research and Design*. 88:1024-1032.

Bajwa D., Pourhashem G., Ullah A., Bajwa S. (2019) A Concise Review of Current Lignin Production, Applications, Products and Their Environmental Impact. *Industrial Crops and Products*. 139:111526.

Baucher M., Monties B., Montagu M.V., Boerjan W. (1998) Biosynthesis and Genetic Engineering of Lignin. *Critical Reviews in Plant Sciences*. 17:125-197.

Baumberger S., Abaecherli A., Fasching M., Gellerstedt G., Gosselink R., Hortling B., Li J., Saake B., De jong E. (2007) Molar Mass Determination of Lignins By Size-exclusion Chromatography: Towards Standardisation of the Method. *Holzforschung*. 61:459-468.

Bellaloui N., Mengistu A., Zobiole L., Shier W.T. (2012) Resistance to Toxin-mediated Fungal Infection: Role of Lignins, Isoflavones, Other Seed Phenolics, Sugars, and Boron in the Mechanism of Resistance to Charcoal Rot Disease in Soybean. *Toxin Reviews*. 31:16-26.

Bernardini J., Cinelli P., Anguillesi I., Coltelli M.B., Lazzeri A. (2015) Flexible Polyurethane

Foams Green Production Employing Lignin Or Oxypropylated Lignin. *European Polymer Journal*. 64: 147-156.

Björkman A. (1954) Isolation of Lignin From Finely Divided Wood with Neutral Solvents. *Nature*. 174:1057-1058.

Boerjan W., Ralph J., Baucher M. (2003) Lignin Biosynthesis. *Annual Review of Plant Biology*. 54:519-546.

Bose S.K., Wilson K.L., Francis R.C., Aoyama M. (1998) Lignin Analysis By Permanganate Oxidation. I. Native Spruce Lignin. *Holzforschung-international Journal of the Biology, Chemistry, Physics and Technology of Wood*. 52:297-303.

Brown W. (1967) Solution Properties of Lignin. Thermodynamic Properties and Molecular Weight Determinations. *Journal of Applied Polymer Science*. 11:2381-2396.

Campbell M.M., Sederoff R.R. (1996) Variation in Lignin Content and Composition (mechanisms of Control and Implications for the Genetic Improvement of Plants). *Plant Physiology*. 110:3-13.

Capanema E.A., Balakshin M.Y., Kadla J.F. (2004) A Comprehensive Approach for Quantitative Lignin Characterization by NMR Spectroscopy. *Journal of Agricultural and Food Chemistry*. 52:1850-1860.

Capanema E.A., Balakshin M.Y., Chen C., Gratzl J.S., Gracz H. (2001) Structural Analysis of Residual and Technical Lignins by 1H-13C Correlation 2D NMR-spectroscopy. *Holzforschung*. 55:302-308.

Capanema E., Balakshin M., Katahira R., Chang H., Jameel H. (2015) How Well Do MWL and CEL Preparations Represent the Whole Hardwood Lignin?. *Journal of Wood Chemistry*

and Technology. 35:17-26.

Cathala B., Saake B., Faix O., Monties B. (2003) Association Behaviour of Lignins and Lignin Model Compounds Studied by Multidetector Size-exclusion Chromatography. *Journal of Chromatography a*. 1020:229-239.

Chang H., Cowling E.B., Brown W. (1975) Comparative Studies on Cellulolytic Enzyme Lignin and Milled Wood Lignin of Sweetgum and Spruce. *Holzforschung-international Journal of the Biology, Chemistry, Physics and Technology of Wood*. 29:153-159.

Chang H., Jiang X. (2020) Biphenyl Structure and Its Impact on the Macromolecular Structure of Lignin: a Critical Review. *Journal of Wood Chemistry and Technology*. 40:81-90.

Chee K. (1987) Novel Approach to Mark-Houwink-Sakurada Constants and Related Parameters of Polystyrene Solutions. *Polymer*. 28:977-979.

Chemin M., Rakotovelo A., Ham-pichavant F., Chollet G., Da silva perez D., Petit-conil M., Cramail H., Grelier S. (2015) Synthesis and Characterization of Functionalized 4-*O*-methylglucuronoxylan Derivatives. *Holzforschung*. 69:713-720.

Chuksanova A., Grushnikov O., Shorygina N. (1961) Heterogeneity of Nitrolignin. *Russian Chemical Bulletin*. 10:1688-1690.

Cinelli P., Anguillesi I., Lazzeri A. (2013) Green Synthesis of Flexible Polyurethane Foams from Liquefied Lignin. *European Polymer Journal*. 49: 1174-1184.

Contreras S., Gaspar A.R., Guerra A., Lucia L.A., Argyropoulos, D.S. (2008) Propensity of lignin to associate: light scattering photometry study with native lignins. *Biomacromolecules*. 9:3362–3369.

Crestini C., Lange H., Sette M., Argyropoulos D.S. (2017) On the Structure of Softwood Kraft

Lignin. *Green Chemistry*. 19:4104-4121.

Crestini C., Melone F., Sette M., Saladino R. (2011) Milled Wood Lignin: a Linear Oligomer. *Biomacromolecules*. 12:3928-3935.

Cui C., Sun R., Argyropoulos D.S. (2014) Fractional Precipitation of Softwood Kraft Lignin: Isolation of Narrow Fractions Common to a Variety of Lignins. *ACS Sustainable Chemistry & Engineering*. 2:959-968.

Culebras M., Beaucamp A., Wang Y., Clauss M.M., Frank E., Collins M.N. (2018) Biobased Structurally Compatible Polymer Blends Based on Lignin and Thermoplastic Elastomer Polyurethane as Carbon Fiber Precursors. *ACS Sustainable Chemistry & Engineering*. 6:8816-8825.

Diamel D. (2010) Overview. In: *Lignin and lignans: Advance in Chemistry*. Eds. Heitner C., Dimmel D., Schmidt J. CRC press, England. pp. Chap 1/1–10.

Dong D., Fricke A.L. (1993) Investigation of optical effect of lignin solution and determination of Mw of kraft lignin by LALLS. *Journal of Applied Polymer Science*. 50:1131–1140.

Dolk M., Pla F., Yan J.F., Mccarthy J.L. (1986) Lignin. 22. Macromolecular Characteristics of Alkali Lignin from Western Hemlock Wood. *Macromolecules*. 19:1464-1470.

Dupont A.L., Harrison G. (2004) Conformation and dn/dC Determination of Cellulose in N,N -dimethylacetamide Containing Lithium Chloride. *Carbohydrate Polymers*. 58:233.

Erickson M., Larsson S., Miksche G.E. (1973) Produkten. Viii.* Zur Struktur Des Lignins Der Fichte. *Acta Chemica Scandinavica*. 27:903-914.

Flory P.J. (1953) Determination of Molecular Weights. In: *Principles of Polymer Chemistry*. Ed. Flory P.J. Cornell University Press, New York. pp. VII-4/308–314.

Fredheim G.E., Braaten S.M., Christensen B.E. (2002) Molecular weight determination of lignosulfonates by size-exclusion chromatography and multi-angle laser light scattering. *Journal of Chromatography a*. 942:191–199.

Gidh A.V., Decker S.R., Vinzant T.B., Himmel M.E., Williford C. (2006) Determination of Lignin by Size Exclusion Chromatography Using Multi Angle Laser Light Scattering. *Journal of Chromatography a*. 1114:10-102.

Glasser W.G., Dave V., Frazier C.E. (1993) Molecular Weight Distribution of (semi-) Commercial Lignin Derivatives. *Journal of Wood Chemistry and Technology*. 13:545-559.

Goring D.A.I. (1971) Polymer properties of lignin and lignin derivatives. In: *Lignins. Occurrence, Formation, Structure, and Reactions*. Eds. Sarkanen, K.V., Ludwig, C.H. Wiley-Interscience, New York. pp. 695–768.

Gross S., Sarkanen K., Schuerch C. (1958) Determinations of Molecular Weight of Lignin Degradation Products by Three Methods. *Analytical Chemistry*. 30:518-521.

Grubisic Z., Rempp P., Benoit H. (1967) A Universal Calibration for Gel Permeation Chromatography. *Journal of Polymer Science Part B: Polymer Letters*. 5:753-759.

Guo X., Condra M., Kimura K., Berth G., Dautzenberg H., Dubin P. (2003) Determination of Molecular Weight of Heparin by Size Exclusion Chromatography with Universal Calibration. *Analytical Biochemistry*. 312:33-39.

Han J., Lim S. (2004) Structural Changes of Corn Starches by Heating and Stirring in DMSO Measured By SEC-MALS-RI System. *Carbohydrate Polymers*. 55:265-272.

Hatakeyama T., Asano Y., Hatakeyama H. (2003) Mechanical and Thermal Properties of Rigid

Polyurethane Foams Derived from Sodium Lignosulfonate Mixed with Diethylen, Triethylene and Polyethylene Glycols. *Macromolecular Symposia*. 197:171-180.

Higuchi T., Ito Y. (1958) Dehydrogenation Products of Coniferyl Alcohol Formed by the Action of Mushroom Phenol Oxidase, Rhus-laccase and Radish Peroxidase. *The Journal of Biochemistry*. 45:575-579.

Hofmann K., Glasser W.G. (1993) Engineering Plastics from Lignin. 22. Cure of Lignin Based Epoxy Resins. *The Journal of Adhesion*. 40:229-241.

Hokputsa S., Jumel K., Alexander C., Harding S.E. (2003) A Comparison of Molecular Mass Determination of Hyaluronic Acid Using SEC/MALLS and Sedimentation Equilibrium. *European Biophysics Journal*. 32:450-456.

Huglin M. (1965) Specific Refractive Index Increments of Polymer Solutions. Part I. Literature Values. *Journal of Applied Polymer Science*. 9:3963-4001.

Jacobs A., Dahlman O. (2000) Absolute Molar Mass of Lignins By Size Exclusion Chromatography and MALDI-TOF Mass Spectroscopy. *Nord Pulp Pap Res J*. 15:120-127.

Johansson A., Aaltonen O., Ylinen P. (1987) Organosolv Pulping—Methods and Pulp Properties. *Biomass*. 13:45-65.

Kadla J., Kubo S., Venditti R., Gilbert R., Compere A., Griffith W. (2002) Lignin-based Carbon Fibers for Composite Fiber Applications. *Carbon*. 40:2913-2920.

Kaneko T., Kaneko D., Wang S. (2010) High-performance Lignin-mimetic Polyesters. *Plant Biotechnology*. 27:243-250.

Katahira R., Nakatsubo F. (2001) Determination of Nitrobenzene Oxidation Products by GC

and 1 H-NMR Spectroscopy Using 5-iodovanillin as a New Internal Standard. *Journal of Wood Science*. 47:378-382.

Kishimoto T., Uraki Y., Ubukata M. (2008) Synthesis of Bromoacetophenone Derivatives as Starting Monomers for β-o-4 Type Artificial Lignin Polymers. *Journal of Wood Chemistry and Technology*. 28:97-105.

Kishimoto T., Uraki Y., Ubukata M. (2006) Chemical Synthesis of β-o-4 Type Artificial Lignin. *Organic & Biomolecular Chemistry*. 4:1343-1347.

Kishimoto T., Uraki Y., Ubukata M. (2008) Synthesis of β-o-4-type Artificial Lignin Polymers and Their Analysis by NMR Spectroscopy. Organic & Biomolecular Chemistry. 6:2982-2987.

Kleen M., Pranovich A., Willför S. (2016) Statistical Modeling of Pressurized Hot-water Batch Extraction (PHWE) to Produce Hemicelluloses with Desired Properties. *Holzforschung*. 70:633-640.

Kulicke W., Kniewske R. (1984) The Shear Viscosity Dependence on Concentration, Molecular Weight, and Shear Rate of Polystyrene Solutions. *Rheologica Acta*. 23:75-83.

Lichtman J.W., Conchello J. (2005) Fluorescence Microscopy. *Nature Methods*. 2:910-919.

Lindberg J.J., Tylli H., Majani C. (1964) Notes on the Molecular Weight and the Fractionation of Lignins with Organic Solvents. *Paperi Ja Puu*. 46:521-526.

Liu W., Fang C., Wang S., Huang J., Qiu X. (2019) High-performance Lignin-containing Polyurethane Elastomers with Dynamic Covalent Polymer Networks. *Macromolecules*. 52:6474-6484.

Lue L. (2000) Volumetric Behavior of Athermal Dendritic Polymers: Monte Carlo Simulation.

Macromolecules. 33:2266-2272.

Lyulin A.V., Adolf D.B., Davies G.R. (2001) Computer Simulations of Hyperbranched Polymers in Shear Flows. *Macromolecules*. 34:3783-3789.

Macfarlane A., Mai M., Kadla J. (2014) Bio-based chemicals from biorefining: Lignin conversion and utilization. In: *Advances in Biorefineries*. Ed. Waldron K. Elsevier, New York. pp. Part II-20/659-692.

Metzger J.O., Bicke C., Faix O., Tuszynski W., Angermann R., Karas M., Strupat K. (1992) Matrix-assisted Laser Desorption Mass Spectrometry of Lignins. *Angewandte Chemie International Edition in English*. 31:762-764.

Michielsen S. (1999) Specific refractive index increments of polymers in dilute solution. In: *Polymer Handbook*, 4th ed. Eds. Brandrup, J., Immergut, E., Grulke, E. Wiley-Interscience, New York. pp. VII/547–628.

Mikame K., Funaoka M. (2006) Polymer Structure of Lignophenol II. *Polymer Journal*. 38:592-596.

Moacanin J., Felicetta V.F., Haller W., Mccarthy J.L. (1955) Lignin. VI. Molecular Weights of Lignin Sulfonates by Light Scattering. *Journal of the American Chemical Society*. 77:3470-3475.

Mourey T., Miller S., Balke S. (1990) Size Exclusion Chromatography Calibration Assessment Utilizing Coupled Molecular Weight Detectors. *Journal of Liquid Chromatography*. 13:435-452.

Muller P.C., Kelley S.S., Glasser W.G. (1984) Engineering Plastics From Lignin. Ix. Phenolic Resin Synthesis and Characterization. *The Journal of Adhesion*. 17:185-206.

Nagatani M., Tsurumaki A., Takamatsu K., Saito H., Nakamura N., Ohno H. (2019) Preparation of Epoxy Resins Derived from Lignin Solubilized in Tetrabutylphosphonium Hydroxide Aqueous Solutions. *International Journal of Biological Macromolecules*. 132:585-591.

Norberg I., Nordström Y., Drougge R., Gellerstedt G., Sjöholm E. (2013) A New Method for Stabilizing Softwood Kraft Lignin Fibers for Carbon Fiber Production. *Journal of Applied Polymer Science*. 128:3824-3830.

Ono Y., Hiraoki R., Fujisawa S., Saito T., Isogai A. (2015) SEC-MALLS Analysis of Wood Holocelluloses Dissolved in 8 % LiCl/1,3-dimethyl-2-imidazolidinone: Challenges and Suitable Analytical Conditions. *Cellulose*. 22:3347-3357.

Pang B., Yang S., Fang W., Yuan T., Argyropoulos D.S., Sun R. (2017) Structure-property Relationships for Technical Lignins for the Production of Lignin-phenol-formaldehyde Resins. *Industrial Crops and Products*. 108:316-326.

Pew J.C. (1963) Evidence of a Biphenyl Group in Lignin1. *The Journal of Organic Chemistry*. 28:1048-1054.

Pierre S., Cyrille R., Isabelle M., Christophe V.A., Alain D. (2003) Light Scattering Studies of the Solution Properties of Chitosans of Varying Degrees of Acetylation. *Biomacromolecules*. 4:1034-1040.

Powell W.J., Whittaker H. (1924) XlII.-the Chemistry of Lignin. Part I. Flax Lignin and Some Derivatives. *Journal of the Chemical Society*. 125:357-364.

Ragauskas A.J., Beckham G.T., Biddy M.J., Chandra R., Chen F., Davis M.F., Davison B.H., Dixon R.A., Gilna P., Keller M. (2014) Lignin Valorization: Improving Lignin Processing in the Biorefinery. *Science*. 344:1246843.

Rezanowich A., Yean W., Goring D. (1964) High Resolution Electron Microscopy of Sodium Lignin Sulfonate. *Journal of Applied Polymer Science*. 8:1801-1812.

Rönnols J., Jacobs A., Aldaeus F. (2017) Consecutive Determination of Softwood Kraft Lignin Structure and Molar Mass from NMR Measurements. *Holzforschung*. 71:563-570.

Saito T., Perkins J.H., Jackson D.C., Trammel E., Hunt M.A., Naskar A.K. (2013) Development of Lignin-based Polyurethane Thermoplastics. *RSC Advances* 3: 21832-21840.

Sarkar S., Adhikari B. (2000) Lignin-modified Phenolic Resin: Synthesis Optimization, Adhesive Strength, and Thermal Stability. *Journal of Adhesion Science and Technology.* 14:1179-1193.

Sasaki C., Wanaka M., Takagi H., Tamura S., Asada C., Nakamura Y. (2013) Evaluation of Epoxy Resins Synthesized from Steam-exploded Bamboo Lignin. *Industrial Crops and Products*. 43:757-761.

Shrotri A., Kobayashi H., Fukuoka A. (2017) Catalytic Conversion of Structural Carbohydrates and Lignin to Chemicals. *Advances in Catalysis*. 60:59-123.

Singh A., Yadav K., Kumar sen A. (2012) Sal (*Shorea Robusta*) Leaves Lignin Epoxidation and Its Use in Epoxy Based Coatings. *American Journal of Polymer Science*. 2:14-18.

Siochi E.J., Ward T.C., Haney M.A., Mahn B. (1990) The Absolute Molecular Weight Distribution of Hydroxypropylated Lignins. *Macromolecules*. 23:1420-1429.

Sjostrom E. (1993) Lignin. In: *Wood Chemistry: Fundamentals and Applications*. Ed. Sjostrom E. Academic Press, California. pp. Chap 4:71-86.

Spatorico A., Coulter B. (1973) Molecular Weight Determinations by Gel-permeation Chromatography and Viscometry. *Journal of Polymer Science Part B: Polymer Physics*.

11:1139-1150.

Sperling L.H. (2005) Dilute Solution Thermodynamics, Molecular Weights, and Sizes. In: *Introduction to Physical Polymer Science*. Ed. Sperling L.H. Wiley-Interscience, New Jersey. pp. Chap 3:110-117.

Sudo K., Shimizu K. (1992) A New Carbon Fiber from Lignin. *Journal of Applied Polymer Science*. 44:127-134.

Taira S., Kurihara M., Koda K., Sugimura K., Nishio Y., Uraki Y. (2019) Tempo-oxidized Cellulose Nanofiber-reinforced Lignin Based Polyester Films as a Separator for Electric Double-layer Capacitor. *Cellulose*. 26:569-580.

Umoren S.A., Solomon M.M. (2016) Polymer Characterization: Polymer Molecular Weight Determination. In: *Polymer Science: Research Advances, Practical Applications and Educational Aspects.* Eds. Vilas A.M.; Martín A.S. Formatex Research Center S.L., Spain. pp:412-419.

Uraki Y., Kubo S., Nigo N., Sano Y., Sasaya T. (1995) Preparation of Carbon Fibers from Organosolv Lignin Obtained By Aqueous Acetic Acid Pulping. *Holzforschung-international Journal of the Biology, Chemistry, Physics and Technology of Wood*. 49:343-350.

Wang L., Aorigele, Sun Y. (2017) Preparation of Iron Oxide Particle-decorated Lignin-based Carbon Nanofibers as Electrode Material for Pseudocapacitor. *Journal of Wood Chemistry and Technology.* 37:423-432.

Wang L., Uraki Y., Koda K., Gele A., Zhou X., Chen F. (2019) Determination of the Absolute Molar Mass of Acetylated Eucalyptus Kraft Lignin By Two Types of Size-exclusion

Chromatography Combined with Multi-angle Laser Light-scattering Detectors. *Holzforschung*. 73:363-369.

Weiss A.R., Cohn-ginsberg E. (1969) A Note on the Universal Calibration Curve for Gel Permeation Chromatography. *Journal of Polymer Science Part C: Polymer Letters*. 7:379-381.

Woerner D.L., Mccarthy J.L. (1988) Lignin. 24. Ultrafiltration and Light-scattering Evidence for Association of Kraft Lignins in Aqueous Solutions. *Macromolecules*. 21:2160-2166.

Wu S., Argyropoulos D. (2003) An Improved Method for Lsolating Lignin in High Yield and Purity. *Journal of Pulp and Paper Science*. 29:235-240.

Yamamoto Y., Cheng N., Koda K., Igarashi K., Tamai Y., Uraki Y. (2017) Association of Amphipathic Lignin Derivatives with Cellobiohydrolase Groups Improves Enzymatic Saccharification of Lignocellulosics. *Cellulose*. 24:1849-1862.

You X., Koda K., Yamada T., Uraki Y. (2015) Preparation of Electrode for Electric Double Layer Capacitor from Electrospun Lignin Fibers. *Holzforschung*. 69:1097-1106.

Zinovyev G., Sulaeva I., Podzimek S., Rössner D., Kilpeläinen I., Sumerskii I., Rosenau T., Potthast A. (2018) Getting Closer to Absolute Molar Masses of Technical Lignins. *Chemsuschem*. 11:3259-3268.

Acknowledgement

I would like to express my great appreciation to the people who have guided and helped me when I studied in Japan as a Ph.D. candidate. First, I would like to thank my supervisor, Prof. Yasumitsu Uraki, for giving me the chance to get in this beautiful campus and study in this great lab. His strict attitude to academic research, distinct and effective teaching style strongly impress me and will have a positive lasting affection in my future. I would also like to thank Dr. Aorigele Gobro, Dr. Keiichi Koda and Dr. Kengo Shigetomi who provided helpful advice and constructive suggestions. My whole doctoral study could not be successfully completed without their guidance and assistance.

I would also like to thank all my lab members who are always helpful when I have some problems in experiments and daily life. Without their company, my life in Japan will not be so happy and colorful. Great thanks are also to our department faculty, staff and fellow students for their well-organized work, friendship, and help. I really appreciate the various activities conducted by our faculty.

Finally, I would like to thank my family who always stand with me and give me the love and support.